This is to certify that the
thesis entitled

A MODIFIED TOPCOLOR MODEL

presented by

Michael Flossdorf

has been accepted towards fulfillment
of the requirements for the

M.S. degree in Department of Physics and Astronomy

Elizabeth H. Simmons
Major Professor's Signature

June 29, 2007
Date

MSU is an affirmative-action, equal-opportunity employer

DATE DUE	DATE DUE	DATE DUE

A MODIFIED TOPCOLOR MODEL

By

Michael Flossdorf

A THESIS

Submitted to
Michigan State University
in partial fulfillment of the requirements
for the degree of

MASTER OF SCIENCE

Department of Physics and Astronomy

2007

Abstract

A MODIFIED TOPCOLOR MODEL

By

Michael Flossdorf

In this thesis we will consider a Topcolor assisted Technicolor model with a flavor universal hypercharge sector. However, before we discuss the details of this model, we will in the first sections give an introduction to basic concepts of spontaneously symmetry breaking and show where they occur in the Standard Model of particle physics. In particular, we will in some detail explain spontaneously symmetry breaking in QCD, since it is considered to be the prototype of *dynamical* spontaneously symmetry breaking. We will then compare it to the symmetry breaking pattern induced by the Higgs sector and use this to motivate the Technicolor approach to go beyond the Standard Model. Then we will address the problems of Technicolor to generate the large top mass and introduce our Topcolor model as a possible solution to this.

After discussing the symmetry breaking pattern and calculating the electroweak parameters in our Topcolor model, we will then look at various experimental and theoretical constraints. We will find that our model is able to sufficiently suppress flavor changing neutral currents and that the largest constraints on our parameter space are due to electroweak precision measurements. We will do a combined fit to all available data at Z pole energies and find that our goodness of fit is comparable to the Standard Model.

Finally, we will also look at Topcolor assisted Technicolor models, which have a flavor non-universal hypercharge sector, like the model proposed by Simmons and Popovic [14] or Hill [10]. In this case we will find that these models are *not* able to fit the data satisfactorily.

ACKNOWLEDGMENTS

I would like to thank my advisors Prof. Elizabeth H. Simmons and Prof. R. Sekhar Chivukula very much for their great support and Felix Braam for many useful discussions. Also, I would like to thank Dr. Kazuhiro Tobe, Baradhwaj Coleppa and Chuan-Ren Chen.

Contents

List of Tables

List of Figures

Chapter 1

Introduction

In this thesis we are considering a modification of a Topcolor assisted Technicolor model which was proposed by Simmons and Popovic [14]. We will introduce a Topcolor model which is flavor universal in the hypercharge sector, but not in the $SU(3)$ (Coloron) sector.

Before we begin to discuss the details of this model, we will give a short introduction to the basic concepts of spontaneously symmetry breaking. We will then apply these concepts to the Standard Model Higgs sector. Afterwards we will discuss in detail the prototype of dynamical spontaneously symmetry breaking: chiral symmetry breaking in QCD. We will then use this to motivate Technicolor models. The lack of a fermion mass generation process will then lead us to Extended Technicolor.

Hereafter we will motivate why Extended Technicolor has a problem with the large top mass and then introduce Topcolor assisted Technicolor models as a possible solution to this problem. In particular we then introduce our modified Topcolor model and its gauge groups and symmetry breaking structure. In the subsequent sections we use the Nambu-Jona-Lasinio approximation to model how the top quark could acquire a mass near its experimental value due to the Topcolor interactions.

One of the main problems of Extended Technicolor is large flavor changing neutral currents. We will therefore start our analysis of the experimental constraints on our Topcolor model by showing that it is possible to sufficiently suppress them in this model. Rather, the most important constraints will be due to electroweak precision tests. Calculating various

observables within the framework of our model will then enable us to do a combined fit to all available LEP (Large Electron Positron Collider) Z pole data to find that our model is able to provide a fit to the data comparable to the Standard Model. We will also calculate the electroweak parameters which sufficiently parameterize universal models beyond the Standard Model and use them to put strong constraints on our parameter space. This analysis will afterwards enable us to place bounds on the masses of the gauge bosons of our model.

Finally we will take a closer look at the Simmons and Popovic Topcolor model [14] and find that due to the flavor non-universality of the hypercharge sector, this model is not able to fit the electroweak data well. The same is true for a Topcolor assisted Technicolor model proposed by Christopher Hill [10], which is flavor non-universal in the hypercharge and in the Coloron sector.

1.1 Symmetries in Field Theory and Quantum Mechanics

Before we start discussing symmetries of the Standard Model (SM), in this section we will derive some technical basic tools which we will need later. In most parts we here follow the excellent lecture given by Edward Farhi [7], but we will also use ref. [15], where a more rigorous treatment is given.

In classical field theory we can have a Lagrangian $\mathcal{L} = \mathcal{L}\left(\phi^i, \partial_\mu \phi^i\right)$ which is a function of a set of space- and time-dependent fields $\phi^i(x^\mu)$ and its derivatives $\partial_\mu \phi^i(x^\mu)$, where $x^\mu = (t, \vec{x})$. The dynamics of the system are then described by the Euler-Lagrange equations of motion:

$$\frac{\partial \mathcal{L}}{\partial \phi^i} - \partial_\mu \frac{\partial \mathcal{L}}{\partial \left(\partial_\mu \phi^i\right)} = 0, \tag{1.1}$$

which extremize the action

$$S\left[\phi^i\right] = \int d^4x \, \mathcal{L}\left(\phi^i, \partial_\mu \phi^i\right). \tag{1.2}$$

We can now consider the following global transformation (i.e. a transformation which has the same form on every point in space-time), which is supposed to be continuous in the parameter α and equal to the identity for $\alpha = 0$:

$$\phi^i(x^\mu) \rightarrow \phi^i(x^\mu, \alpha). \tag{1.3}$$

Infinitesimally (meaning α small), this transformation will look like

$$\phi^i \rightarrow \phi^i + \alpha\delta\phi^i. \tag{1.4}$$

All transformations we will need will be linear and therefore have the general form

$$\delta\phi^i = iT^{ij}\phi^j, \tag{1.5}$$

where T is supposed to be hermitean and we have put in the imaginary unit i for conventional reasons. Note that if we know the infinitesimal transformation to be (1.5), we can always construct the corresponding finite transformation by writing

$$\phi^i \rightarrow [\exp(i\alpha T)]_{ij}\,\phi^j. \tag{1.6}$$

A transformation like (1.4) is now called a symmetry, if the transformed fields obey the same equation of motion as the untransformed. The latter condition is equivalent to have an unchanged action S after the transformation:

$$S\left[\phi^i\right] = S\left[\phi^i + \alpha\delta\phi^i\right]. \tag{1.7}$$

This in turn means that the Lagrangian is only allowed to change by a surface term (which may be zero):

$$\delta\mathcal{L} = \partial_\mu\Lambda^\mu. \tag{1.8}$$

If this equation holds (meaning our continuous transformation is indeed a symmetry), we find that the famous Noether current

$$j^\mu = \frac{\partial\mathcal{L}}{\partial\left(\partial_\mu\phi^i\right)}\delta\phi^i - \Lambda^\mu \tag{1.9}$$

is a conserved quantity, meaning

$$\partial_\mu j^\mu = 0. \tag{1.10}$$

This also tells us that

$$Q \equiv \int d^3x \; j^0 \tag{1.11}$$

is a constant of motion: $\frac{dQ}{dt} = 0$. This constant of motion is sometimes called *charge*.

To be able to generalize some of the above results to quantum field theory, we also define the canonical momentum field

$$\pi^\mu = \frac{\partial \mathcal{L}}{\partial \left(\partial_\mu \phi^i\right)}. \tag{1.12}$$

Then the conserved current in the case of a linear transformation will take the form

$$j^\mu = i\pi_i^\mu T^{ij}\phi^j, \tag{1.13}$$

if the surface term vanishes identically: $\delta\mathcal{L} = 0$. All symmetry transformations we consider will be of the form of eqn. (1.13).

According to the procedure of canonical quantization, we can now promote the fields ϕ^i and π^i to operators and impose the following commutation relations:

$$\begin{aligned} \left[\phi^i(x^\mu)\,,\pi_j(y^\mu)\right] &= i\delta_j^i\delta^3(\vec{x}-\vec{y})\,, \\ \left[\phi^i(x^\mu)\,,\phi^j(y^\mu)\right] &= 0, \\ \left[\pi_i(x^\mu)\,,\pi_j(y^\mu)\right] &= 0. \end{aligned} \tag{1.14}$$

Inspired by eqn. (1.11), we may define the *charge operator* for the case of a linear transformation

$$Q(t) = i\int d^3x \; \pi_i(x^\mu)\, T^{ij}\phi^j(x^\mu)\,. \tag{1.15}$$

Using the commutation relations (1.14), we find

$$\begin{aligned} \left[Q(t)\,,\phi^k(y^\mu)\right] &= T^{kj}\phi^j(y^\mu) = -i\delta\phi^k(y^\mu) \text{ and} \\ \left[Q(t)\,,\pi_k(y^\mu)\right] &= -T^{ik}\pi_i(y^\mu) = -i\delta\pi_k(y^\mu)\,. \end{aligned} \tag{1.16}$$

Since the Hamiltonian H can only be dependent on powers of ϕ^i and π^i, we also conclude

$$[Q(t)\,, H] = -i\delta H. \tag{1.17}$$

Now we can read off the desired result: If the transformation induced by T^{ij} is a symmetry of the Hamiltonian, we have $\delta H = 0$, which means that in this case Q commutes with the Hamiltonian and we found the quantum field theory analogue to eqn. (1.11):

$$\frac{dQ(t)}{dt} = 0. \tag{1.18}$$

We summarize: Let G be a (symmetry) group of continuous transformations, $\delta\phi = i\alpha T^{ij}\phi^j$, where T^{ij} is the matrix representation of the group generator T fulfilling $\exp(-\alpha T) \in G$. If the action S is invariant under the transformations in G, then the charge operator Q defined in (1.15) is conserved (i.e. time independent) and generates group transformations in the sense of eqn. (1.16), which we can readily identify with the infinitesimal form of the finite transformation

$$\phi(x^\mu) \to e^{i\alpha Q}\phi(x^\mu)\,e^{-i\alpha Q}. \tag{1.19}$$

Note that we can easily generalize our result to n dimensional symmetry groups, which have n generators T^a and are continuous in the n parameters α^a: $\exp(-i\alpha^a T^a) \in G$.

In quantum field theory, the vacuum $|0\rangle$ is defined to be the state with the lowest energy. If we set this energy to zero, we have

$$P^\mu\,|0\rangle = 0. \tag{1.20}$$

where P^μ is the momentum operator.

If we let G be the symmetry of the action, we can now ask how the vacuum state $|0\rangle$ transforms under G and distinguish two types of realizations of this symmetry.

In the *Wigner realization* of the symmetry, the vacuum possesses the same symmetry as the action, i.e.

$$|0\rangle \to e^{-i\alpha^a Q^a}\,|0\rangle = |0\rangle\,, \tag{1.21}$$

which is equivalent to

$$Q^a |0\rangle = 0, \tag{1.22}$$

for all a. Then we also have

$$\langle 0| \delta\phi |0\rangle = \langle 0| [iQ^a, \phi] |0\rangle = 0, \tag{1.23}$$

for all fields ϕ in the action. Note that here and in the following we omit the superscript i. We will also later often use the short form $\langle\phi\rangle$ instead of $\langle 0| \phi |0\rangle$.

The more interesting case for us in this thesis will be the *Nambu-Goldstone realization*, where there exists some field ϕ with

$$\langle 0| \delta\phi |0\rangle \neq 0, \tag{1.24}$$

which means that the vacuum $|0\rangle$ does *not* respect the same symmetry as the action:

$$Q^a |0\rangle \neq 0, \tag{1.25}$$

for at least one generator Q^a. In this case we say that the symmetry is *spontaneously broken* and all Q^a for which eqn. (1.25) is true, are referred to as being *broken* generators.

So in the latter case we can have a formally conserved current and a conserved charge from Noether's theorem at the Lagrangian level, but the vacuum does not respect the symmetry of the action and therefore all the other states in the Fock space built from the vacuum state will not either. Thus there will be no apparent conservation of the charge which corresponds to the broken generator.

Since spontaneous symmetry breaking occurs only if $\langle 0| \delta\phi |0\rangle \neq 0$, we will call $\langle 0| \delta\phi |0\rangle$ an *elementary order parameter*. We can also have *composite order parameters*, $\delta \langle 0| \phi_1 \dots \phi_n |0\rangle$, signalizing the spontaneous break down of a symmetry. This will become important when we consider spontaneous symmetry breaking in Quantum Chromo Dynamics (QCD) in section 1.3.

We will now show that the existence of a non-zero order parameter alone will lead to the occurrence of massless particles in the spectrum, called Nambu-Goldstone bosons. The

theorem which states the existence of those particles is called the *Goldstone theorem*. We will here follow [7] and prove the following version of this theorem:

> Let the action of a quantum field theory be invariant under a continuous symmetry which is associated with a conserved current j^μ. If except for the vacuum, every state has $p^\mu p_\mu \geq \epsilon$ for some $\epsilon > 0$, then $\langle 0| \delta\phi(y) |0\rangle = 0$ for all fields $\phi(y)$.

Proof. We will look at the matrix element $\langle 0| j_\mu(x)\, \phi(y) |0\rangle$ and use eqn. (1.20) after we insert a complete set of physical states:

$$\begin{aligned}
\langle 0| j_\mu(x)\, \phi(y) |0\rangle &= \sum_n \langle 0| j_\mu(x) |n\rangle \langle n| \phi(y) |0\rangle \\
&= \sum_n \langle 0| e^{iP\cdot x} j_\mu(0)\, e^{-iP\cdot x} |n\rangle \langle n| e^{iP\cdot y} \phi(0)\, e^{-iP\cdot y} |0\rangle \\
&= \sum_n \langle 0| j^\mu(0) |n\rangle \langle n| \phi(0) |0\rangle\, e^{ip_n\cdot(y-x)} \\
&= \int d^4k \sum_n \delta^4(k - p_n) \langle 0| j_\mu(0) |n\rangle \langle n| \phi(0) |0\rangle\, e^{ik\cdot(y-x)}.
\end{aligned} \tag{1.26}$$

We will now assume that j_μ is a Lorentz vector and that ϕ is a Lorentz scalar.[1] This enables us to define a function $\rho(k^2)$ by

$$k_\mu \rho\left(k^2\right) \equiv \sum_n \delta^4(k - p_n) \langle 0| j_\mu(0) |n\rangle \langle n| \phi(0) |0\rangle . \tag{1.27}$$

in this sum we cannot get a contribution from the vacuum, since $\langle 0| j_\mu(0) |0\rangle$ must vanish (also due to Lorentz invariance). By assumption, there is no other state with $p_n \cdot p_n < \epsilon$ for $p_n < \epsilon$ so from eqn. (1.27) we see that $\rho(k^2) = 0$ for $k^2 < \epsilon$.

Using (1.27) we may write:

$$\langle 0| j_\mu(x)\, \phi(y) |0\rangle = \int d^4k\, k_\mu \rho\left(k^2\right) e^{ik\cdot(y-x)}. \tag{1.28}$$

[1] Note that we might run into a problem here, if we consider local gauge theories, where depending on the gauge we choose, we might loose manifest Lorentz invariance (for example in Coulomb gauge in QED). This exception will be important in understanding the Higgs mechanism, as we describe later.

Due to current conservation we have $\partial_\mu j^\mu(x) = 0$ and thus $k^2\rho(k^2) = 0$. If $k^2 > 0$ this implies $\rho(k^2) = 0$.

Since we already found $\rho(k^2) = 0$ for $k^2 < \epsilon$, we infer $\rho(k^2) = 0$ for all k^2, which enables us to write

$$\langle 0| j_\mu(x)\, \phi(y) |0\rangle = 0. \tag{1.29}$$

And by the same arguments,

$$\langle 0| \phi(y)\, j_\mu(x) |0\rangle = 0. \tag{1.30}$$

Combining the last two equations yields

$$\int d^3x \langle 0| [j_0(x)\,, \phi(y)] |0\rangle = 0 \tag{1.31}$$

or

$$\langle 0| \delta\phi(y) |0\rangle = 0. \tag{1.32}$$

□

From the contraposition, we thereby prove the existence of a state with $p_\mu p^\mu = 0$ if the order parameter $\langle 0| \delta\phi(0) |0\rangle$ *does not vanish.* This state is the Goldstone boson which we denote π (not to be confused with the canonical momentum). If we now had $\langle 0| j_\mu(x) |\pi(p)\rangle = 0$, we could separate the Goldstone boson state from the sum over the rest of the physical states in (1.26) and by the same arguments show that $\langle 0| \delta\phi(0) |0\rangle = 0$, contradicting to what we just proved. We thus also know $\langle 0| j_\mu(x) |\pi(p)\rangle \neq 0$.

Analyzing the Lorentz structure of this term, we find that it must be proportional to p_μ, since a x_μ term would imply a vanishing coupling of the Goldstone boson for $x_\mu = 0$. By the same argument we cannot have a term proportional to x^2. The only scalar left we can construct with p^μ and x^μ is $x \cdot p$. Also wanting to have a vanishing four-divergence we may thus parameterize the coupling of the Goldstone boson to the broken current in the following way:

$$\langle 0| j_\mu(x) |\pi(p)\rangle = if p_\mu e^{ip\cdot x}, \tag{1.33}$$

where f denotes the strength of the coupling. In the case of more than one broken generator of the symmetry group G of the action, we will get one Goldstone boson for each broken generator.

1.2 Spontaneous Symmetry Breaking in the Standard Model Higgs Sector

We will in this section discuss the Higgs sector of the Standard Model (SM) Lagrangian and thereby give an introduction to linear and non-linear sigma models, which we will need later. Apart from this, it is worthwhile discussing the Higgs sector in some detail, because we will later find that more general models like Technicolor have a low energy effective Lagrangian with exactly the same structure, but need not have an elementary Higgs boson. A much more detailed treatment of sigma fields can be found in ref. [7] and [11], which we are partly following here.

Let us start by introducing a complex scalar field ϕ, which transforms as a doublet under $SU(2)_L$ and to which we also assign the (hyper-) charge $\phi_Y = 1/2$ under a $U(1)_Y$ group. We now write down the following Lagrangian, which is invariant under the global transformation $SU(2)_L \otimes U(1)_Y$:

$$\mathcal{L} = \partial_\mu \phi^\dagger \partial^\mu \phi - \lambda \left(\phi^\dagger \phi - \frac{v^2}{2} \right)^2 , \tag{1.34}$$

where we introduced the famous mexican hat potential

$$V(\phi) = \lambda \left(\phi^\dagger \phi - \frac{v^2}{2} \right)^2 . \tag{1.35}$$

The vacuum corresponds to the lowest energy state, which in this case means that the vacuum expectation value (vev) of ϕ is non-vanishing:

$$\langle 0 | \phi | 0 \rangle = e^{i\alpha^a \tau^a} \begin{pmatrix} 0 \\ v/\sqrt{2}, \end{pmatrix} , \tag{1.36}$$

where the α^a are arbitrary real parameters and $\tau^a \equiv \sigma^a/2$ with σ^a being the Pauli matrices (the τ^a form a matrix representation of the group generators of $SU(2)$). The lowest energy

state is degenerate and we could choose any factors α^a. For convenience we will choose $\alpha^a = 0$. The Lagrangian we wrote down is invariant under $SU(2)_L \otimes U(1)_Y$, but the vacuum expectation value (1.36) is not. We can see this explicitly:

$$\langle 0|\,\phi\,|0\rangle \to e^{i\theta^a\tau^a} e^{i\theta' Y}\,\langle 0|\,\phi\,|0\rangle = e^{i\theta^a\tau^a} e^{i\theta'\frac{1}{2}} \begin{pmatrix} 0 \\ v/\sqrt{2} \end{pmatrix} \neq \begin{pmatrix} 0 \\ v/\sqrt{2} \end{pmatrix}.$$

We thus have a non zero (elementary) order parameter signaling the spontaneous breakdown of a symmetry. We should be a little more careful: The above vev is actually invariant under the transformation $\tau_3 + Y$, which means, that this generator is unbroken. We thus expect three linearly independent broken generators (τ_1, τ_2, $\tau_3 - Y$) and therefore three massless Nambu-Goldstone bosons.

We can now choose to parameterize the four degrees of freedom of ϕ in terms of four real fields in the following way:

$$\phi = \frac{1}{\sqrt{2}} \begin{pmatrix} i\pi_1 + \pi_2 \\ \sigma - i\pi_3 \end{pmatrix}. \tag{1.37}$$

If we now let $\langle\sigma\rangle = v$ and $\langle\vec{\pi}\rangle = 0$, we reproduce (1.36). Let us also introduce $h \equiv \sigma - v$. Then $\langle h\rangle = 0$. Plugging in eqn. (1.37) into the Lagrangian (1.34) yields

$$\mathcal{L}_{\text{s.o.}} = \frac{1}{2}\left(\partial_\mu h \partial^\mu h + \partial_\mu \vec{\pi} \partial^\mu \vec{\pi}\right) - \lambda v^2 h^2, \tag{1.38}$$

where we also assumed only small oscillations around the lowest energy configuration and therefore expanded around the vacuum configuration $\langle\sigma\rangle = v$ and $\langle\vec{\pi}\rangle = 0$. Our particle spectrum thus contains a massive particle h, the Higgs particle, and three massless fields $\vec{\pi}$, which can readily be identified with the three Nambu-Goldstone bosons.

Before we promote the global $SU(2)_L \otimes U(1)_Y$ symmetry to a local one and thereby reproduce the SM Higgs sector, we introduce the following matrix field

$$\Sigma \equiv \left(i\sigma_2\phi^*, \phi\right) = \frac{1}{\sqrt{2}}\left(\sigma + i\pi^a\sigma^a\right), \tag{1.39}$$

where we used the ϕ field parameterization of (1.37). We also have

$$\langle\Sigma\rangle = \frac{v}{\sqrt{2}}. \tag{1.40}$$

where we omitted the unity matrix. The Lagrangian (1.34) now reads

$$\mathcal{L} = \frac{1}{2}\,\mathrm{Tr}\left[\partial_\mu \Sigma^\dagger \partial^\mu \Sigma\right] - \frac{\lambda}{4}\left[\mathrm{Tr}\,\Sigma^\dagger\Sigma - v^2\right]^2 \tag{1.41}$$

With the help of the identity $\sigma^2\,(\sigma^a)^*\,\sigma^2 = -\sigma^2$ of the Pauli matrices, we can see that if ϕ is a doublet under $SU(2)_L$, so is $i\sigma^2\phi^*$. Thus we have $\Sigma \to A_L\,\Sigma$, with $A_L \in SU(2)$, $A_L = \exp\left(\theta_L^a \tau^a\right)$.

But the way we have written the Lagrangian in (1.41) reveals another symmetry: It is also invariant under $\Sigma \to \Sigma\,A_R^\dagger$, with $A_R = \exp\left(\theta_R^a \tau^a\right)$ and A_R being element of another group, which we denote $SU(2)_R$. So under the two global $SU(2)$ groups, Σ transforms in the following way:

$$\Sigma \to A_L \Sigma A_R^\dagger. \tag{1.42}$$

It is now easy to see that $U(1)_Y$ is a subgroup of $SU(2)$: If ϕ has hypercharge $1/2$, $i\sigma_2\phi$ has hypercharge $-1/2$ and so Σ transforms under $U(1)_Y$ in the following way: $\Sigma \to \Sigma\,e^{-\tau_3 Y \theta_Y}$.

The vacuum expectation value (vev) $\langle\Sigma\rangle$ is *not* invariant under $SU(2)_L \otimes SU(2)_R$. But we see that it is invariant under a simultaneous left and right transformation with $\theta_L = \theta_R$ and we denote the corresponding subgroup $SU(2)_V$. The transformations belonging to this subgroup of $SU(2)_L \otimes SU(2)_R$ are called vector transformations. Thus this subgroup remains unbroken. Plugging $\Sigma = \frac{1}{\sqrt{2}}\left(\sigma + i\sigma^a\tau^a\right)$ into eqn. (1.42) and setting $A_L = A_R$, we see that the pion fields π^a transform as a triplet under the unbroken group $SU(2)_V$ whereas the sigma field behaves as a scalar.

The generators of the orthogonal transformation, under $\theta_L = -\theta_R$, are broken. So the vev of the Σ field spontaneously broke $SU(2)_L \otimes SU(2)_R$ down to $SU(2)_V$ and we again see that we must have three Nambu-Goldstone bosons belonging to the three broken generators of $SU(2)_A$.

What we just discussed is the *linear sigma model* for the ungauged Higgs sector of the SM. In the SM $SU(2)_L \otimes U(1)_Y$ is gauged (meaning it is a local symmetry). So the $U(1)_Y$ subgroup of $SU(2)_R$ becomes gauged.

Let us introduce the so called moose notation to illustrate this [8]. This notation allows us to illustrate the symmetry breaking mechanism at the scale $v/\sqrt{2}$ at a glance. Fig. 1.1 shows this for our example. The dashed circle on the right hand side illustrates that we gauged a $U(1)$ subgroup of the global $SU(2)_R$ and the arrow indicates which group is assumed to transform as the right handed group.

In general, sigma models are used to write down an effective low energy Lagrangian which implements the desired pattern of symmetry breaking. We will use this in section 1.3 and later also to model the symmetry breaking structure of the Topcolor model we are going to introduce.

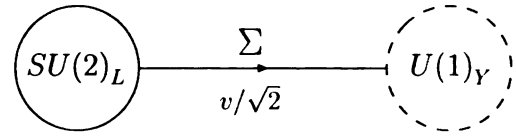

Figure 1.1. The Standard Model symmetry breaking structure illustrated in moose notation.

Concentrating just on the gauged groups (meaning to leave $SU(2)_R$ aside for the moment), we have the following symmetry breaking structure: $SU(2)_L \otimes U(1)_Y \rightarrow U(1)_{\text{em}}$. So the unbroken group belonging to the generator $\tau_3 + Y$ remains unbroken and is identified with the gauge group of electromagnetism $U(1)_{\text{em}}$.

Since we know how the Σ field transforms, we can write down its $SU(2)_L \otimes U(1)_Y$ gauge covariant derivative:

$$D_\mu \Sigma = \partial_\mu \Sigma + igW_\mu^a \tau^a \Sigma - ig' B_\mu \Sigma \frac{\tau_3}{2} \tag{1.43}$$

The gauged Lagrangian now becomes

$$\mathcal{L} = \frac{1}{2} \operatorname{Tr}\left[D_\mu \Sigma^\dagger D^\mu \Sigma\right] - \frac{\lambda}{4}\left[\operatorname{Tr} \Sigma^\dagger \Sigma - v^2\right]^2. \tag{1.44}$$

Our goal is now to write down an effective Lagrangian, which only models the pion degrees of freedom and does not need the h field. Above, we found the mass of the h field

to be $m_h^2 = 2\lambda v^2$. We can now eliminate the h degree of freedom by making this mass infinitely heavy by taking $\lambda \to \infty$. Inspecting the Lagrangian (1.44) we see that

$$\mathrm{Tr}\,\Sigma^\dagger\Sigma - v^2 = 0 \tag{1.45}$$

has to be satisfied to avoid an infinite potential term. Using eqn. (1.39) we find $\Sigma^\dagger\Sigma = \sigma^2 + \vec{\pi}^2$ and furthermore $\det\Sigma = \sigma^2 + \vec{\pi}^2$, so Σ is proportional to a special unitary matrix, which we denote U. We thus see that we can indeed satisfy (1.45) if we set $\Sigma = v/\sqrt{2}\,U$. We can now write U in the following way:

$$U = e^{i\tau^a\pi'^a/v} \quad \text{with} \quad \langle U\rangle = 1. \tag{1.46}$$

Note that compared to eqn. (1.39) we here parameterized the pion degrees of freedom differently by performing a so called *polar decomposition.* Also note that we need v in the denominator of the exponent to get the dimensions right.

We thus finally found

$$\mathcal{L} = \frac{v^2}{4}\,\mathrm{Tr}\left[D_\mu U^\dagger D^\mu U\right], \tag{1.47}$$

which is the Lagrangian of a non-linear sigma model, which also models the desired symmetry breaking, but does not introduce a physical Higgs particle. We should note that contrary to the linear sigma model, the non-linear sigma model is not renormalizable. But nevertheless we can use it to write down low-energy effective Lagrangians.

Generation of Masses in the SM

So far we did not explain why the Standard Model needs the Higgs sector. We will briefly do this now. But since the mass generation of the Standard Model gauge bosons $W^\pm$ and Z due to the non-zero vev of the Higgs particle[2] is analogous to what we will discuss in section 2.3, we will not discuss it here.

The SM model is a chiral theory, meaning that it distinguishes between left- and right-handed fields by assigning different charges to them. Every Dirac field operator describing

[2]In our notation $\langle h\rangle = 0$ only holds, because we already shifted it by v.

a fermion can be split into left- and right-handed pieces by applying the corresponding projection operators, which are defined as $P_L \equiv \frac{1}{2}(1-\gamma_5)$ and $P_R \equiv \frac{1}{2}(1+\gamma_5)$. A fermion mass term now is proportional to $\bar{\psi}\psi = \bar{\psi}_L\psi_R + \bar{\psi}_R\psi_L$ and can therefore not be gauge invariant, because ψ_L and ψ_R belong to different $SU(2)$ representations (and also have different hypercharges).

But with the sigma field of the Lagrangian from eqn. (1.44) we can write down the following Yukawa coupling term which respects all symmetries:

$$\mathcal{L}_Y = \tilde{\lambda}\bar{\psi}_L\Sigma\psi_R + \text{h.c.}, \tag{1.48}$$

where

$$\tilde{\lambda} \equiv \begin{pmatrix} \lambda_u & 0 \\ 0 & \lambda_d \end{pmatrix}$$

with the Yukawa coupling constants λ_u and λ_d and $\psi \equiv (u, d)$. Let us now repeat the polar decomposition we did above, but this time for the linear sigma model, thus keeping the Higgs field h degree of freedom:

$$\Sigma = \frac{1}{\sqrt{2}}(v + h(x))\, e^{i\tau^a \pi(x)^a}, \tag{1.49}$$

where we explicitly wrote the space-time dependence of the fields. Since we are dealing with a local gauge theory, we can now pick a specific gauge, the so called *unitary gauge*, and transform the Σ field:

$$\Sigma \rightarrow e^{-i\tau^a \pi(x)^a}\Sigma = \frac{1}{\sqrt{2}}(v + h(x)). \tag{1.50}$$

Which means that we "gauged away" the pion fields. The pion degrees of freedom manifest themselves in the additional longitudinal degree of freedom of the massive gauge bosons. It is common to say that the Nambu-Goldstone bosons are "eaten" by the gauge bosons to give them masses.

Coming back to the problem of fermion mass generation, we rewrite the Yukawa coupling term (1.48) in the specific gauge we picked:

$$\mathcal{L}_Y = \frac{\lambda_u v}{\sqrt{2}}\bar{u}_L u_R + \frac{\lambda_d v}{\sqrt{2}}\bar{d}_L d_R + \text{h.c.}. \tag{1.51}$$

So this way we were able to write down a mass term without destroying gauge invariance.

Since $v = 246$ GeV, but for example the electron mass is only 511 keV, the Yukawa coupling constants for the different particles of the SM have to be very small. This is viewed as one of the shortcomings of the SM. Also, the Yukawa couplings are just introduced by hand to match the measured fermion masses, but do not evolve from any dynamics. As we will see, this is contrasting to the goal of Extended Technicolor.

1.3 Spontaneous Symmetry Breaking in QCD

QCD is a non-abelian gauge theory. We thus have asymptotic freedom at high energies on the one hand, and confinement at low energies on the other hand. This is manifest in the coupling constant α_S of QCD, whose running as a function of the energy scale μ is described by the beta function. For a QCD like non-abelian gauge theory with n_f quark flavors and N colors the beta function reads

$$\beta(\alpha) = \mu \frac{\partial \alpha}{\partial \mu} = \frac{\alpha^2}{\pi} \left(-\frac{11N}{6} + \frac{n_f}{3} \right), \tag{1.52}$$

to first non-trivial order in α. For QCD $N = 3$ and $n_f = 6$ which yields a negative beta function and therefore a decreasing coupling constant for increasing energy scales. This also means that QCD becomes strong, meaning non-perturbative at small energies. This causes the well-known hadronization at low energies.

We will now follow the discussion of ref. [7] and again also use ref. [11] and [15]. We start by writing down the Lagrangian of QCD, at first for a single quark flavor of mass m:

$$\mathcal{L} = \bar{q}_c i\gamma^\mu D_\mu^{cc'} q_{c'} - \frac{1}{2} \operatorname{Tr} F_{\mu\nu} F^{\mu\nu} - m\, \bar{q}_c q_c, \tag{1.53}$$

with the gauge covariant derivative

$$D_\mu^{cc'} = \partial_\mu \delta^{cc'} + i \frac{g_S}{2} G_\mu^a \lambda_{cc'}^a \tag{1.54}$$

and the field tensor

$$F_{\mu\nu} = \partial_\mu A_\nu - \partial_\nu A_\mu + i g_S \left[A_\mu, A_\nu \right], \tag{1.55}$$

where $G_\mu \equiv G^a_\mu \lambda^a/2$, with the Gell-Mann matrices λ^a which form a matrix representation of the $SU(3)$ group generators. Here we explicitly wrote down the color indices c and c' to clearly distinguish the local color symmetry from the global flavor symmetry we will look at in the following.

Compared to the typical[3] scale of QCD of around 200 MeV, the up and down quark masses of a few MeV are small and we can start by treating them as being massless. Suppressing the color indices from now on, we can write down the QCD Lagrangian for the two flavors:

$$\mathcal{L} = \sum_{i=1}^{2} \bar{q}_i i \not{D} q_i - \frac{1}{2} \operatorname{Tr} F_{\mu\nu} F^{\mu\nu}. \tag{1.56}$$

Since we set the masses of the quarks to zero, the left- and right-handed parts of the quark fields do not mix (compare to eqn. (1.51)). Noting that $\gamma_5^\dagger = \gamma_5$ and that γ_5 in the projection operators anti-commute with the γ_μ in the QCD Lagrangian, we see that in massless QCD left- and right-handed fields can indeed be treated as being independent:

$$\mathcal{L} = \sum_{i=1}^{2} \left(\bar{q}_{iL} i \not{D} q_{iL} + \bar{q}_{iR} i \not{D} q_{iR} \right) - \frac{1}{2} \operatorname{Tr} F_{\mu\nu} F^{\mu\nu}. \tag{1.57}$$

This Lagrangian has the *global* symmetry

$$\begin{pmatrix} u_L \\ d_L \end{pmatrix} \to U_L \begin{pmatrix} u_L \\ d_L \end{pmatrix}, \quad \begin{pmatrix} u_R \\ d_R \end{pmatrix} \to U_R \begin{pmatrix} u_R \\ d_R \end{pmatrix}, \tag{1.58}$$

with U_L and U_R being arbitrary unitary matrices. Thus we have the global *flavor* symmetry $SU(2)_L \otimes SU(2)_R \otimes U(1)_L \otimes U(1)_R$, called *chiral symmetry*. Using (1.13) we can write down the associated Noether currents:

$$\begin{aligned} j^\mu_L &= \bar{q}_L \gamma^\mu q_L, & j^\mu_R &= \bar{q}_R \gamma^\mu q_R, \\ j^{\mu a}_L &= \bar{q}_L \gamma^\mu \tau^a q_L, & j^{\mu a}_R &= \bar{q}_R \gamma^\mu \tau^a q_R, \end{aligned} \tag{1.59}$$

where $q \equiv \begin{pmatrix} u \\ d \end{pmatrix}$.

The most important feature of QCD for us is now that the chiral symmetry of QCD is believed[4] to be spontaneously broken at low energies by the formation of a quark anti-quark

[3] With typical scale we here mean the approximative scale where QCD becomes strong.

[4] So far there is no rigorous proof for this within the framework of QCD.

condensate:

$$\langle \bar{q}_L q_R \rangle \neq 0. \tag{1.60}$$

The non-vanishing of this vev has to be clearly distinguished from the process of hadronization: The occurrence of mesons consisting of quark anti-quark bound states below some energy scale does not mean that (1.60) has to hold.

Since $q\bar{q} = \bar{q}_L q_R + \bar{q}_R q_L$, $\langle \bar{q}q \rangle$ is not invariant under the full symmetry group of the Lagrangian and due to (1.60) we thus have a non-vanishing composite order parameter signalizing the spontaneous break down of the chiral symmetry.

Noting

$$\langle \bar{q}_L q_R \rangle \to e^{-i\tau^a \theta_L^a} e^{i\tau^a \theta_R^a} \langle \bar{q}_L q_R \rangle, \tag{1.61}$$

we see that again not all symmetry generators are broken. The vev $\langle \bar{q}q \rangle$ is invariant if we transform the left- and right-handed fields in the same way, meaning $\theta_L = \theta_R$. The corresponding symmetry group is called the vector group $SU(2)_V$. Broken are the so called axial transformations, which transform left-handed fields opposite to right-handed: $\theta_L = -\theta_R$.

Recalling the definition of the projection operators from last section, we thus identify the currents belonging to the broken generators to be the axial-vector current

$$j^{\mu 5a} = j_R^{\mu a} - j_L^{\mu a} = \bar{q}\gamma^\mu \gamma^5 \tau^a q. \tag{1.62}$$

Note that we will in this discussion ignore the axial $U(1)$ group, which we could recognize to be spontaneously broken by the same argument. A more careful (quantum field theoretically) analysis shows that this symmetry is not spontaneously broken, but that the conservation of the corresponding axial current $j^{\mu 5}$ is actually spoiled by anomalies, see [3].

Using the Goldstone theorem, we expect three massless pions π^a coupling to the broken currents:

$$\langle 0 | \, j^{\mu 5a}(0) \, | \pi^b(q) \rangle = i f_\pi \delta^{ab} q^\mu. \tag{1.63}$$

where f_π is called the pion decay constant[5]. From this we infer that since the currents $j^{\mu 5a}$ transform as a triplet under $SU(2)$, so do the the pion fields. We more generally can identify the pions to have the same quantum numbers as $\bar{q}i\gamma_5\tau^a q$ since $\langle 0|\,\bar{q}i\gamma_5\tau^a q\,|\pi^a\rangle \neq 0$. In that sense we can write

$$\pi^a \sim \bar{q}i\gamma_5\tau^a q, \tag{1.64}$$

implying that the pion is a composite quark anti-quark state. We can now take into account the small masses of the up and down quark in the QCD Lagrangian by adding the following mass term

$$\mathcal{L}_{\text{mass}} = \bar{q}_L M q_r + \bar{q}_R M q_L, \tag{1.65}$$

where

$$M = \begin{pmatrix} m_u & 0 \\ 0 & m_d \end{pmatrix}.$$

This term explicitly breaks the axial part of $SU(2)$ at the Lagrangian level (and if we set $m_u \neq m_d$ also $SU(2)_V$), so we would not expect (massless) Nambu-Goldstone bosons (NGB) in the spectrum, since the corresponding axial current is no longer conserved. But in the limit as the quark masses go to zero, we have exactly massless NGB. So in the real world we expect light NGB, called Pseudo-Nambu-Goldstone bosons (PNGB), which form a triplet under $SU(2)$.

These PNGB were identified with the three lightest mesons, the QCD pions. We could well have treated the strange quark as massless, too, and then would have found eight PNGB, transforming as an octet of flavor $SU(3)$. These PNGB would also be composite and could have been identified with the Kaons and the η of the meson spectrum. It is a little more difficult to relate the Higgs analogue σ field to a particle in the spectrum, but it is often regarded as a very broad resonance, see ref. [15].

We would now like to find an effective Lagrangian describing the QCD chiral symmetry breaking. This effective Lagrangian must contain three pions transforming as a triplet under

[5]See [7] for the relation between f_π and pion decays.

$SU(2)$ and a scalar field σ with $\langle\sigma\rangle \neq 0$. We already found in section 1.2 that the sigma model Lagrangian, eqn. (1.41), has exactly this properties. Thus we write:

$$\mathcal{L} = \frac{1}{2}\,\mathrm{Tr}\left[\partial_\mu \Sigma^\dagger \partial^\mu \Sigma\right] - \frac{\lambda}{4}\left[\mathrm{Tr}\,\Sigma^\dagger\Sigma - f^2\right]^2, \tag{1.66}$$

with $\Sigma \equiv \frac{1}{\sqrt{2}}(\sigma + i\pi^a\tau^a)$. We now need to figure out what f is. Working out the (axial) Noether current $j^{\mu 5a}$, by using (1.13), and calculating $\langle 0|\, j^{\mu 5a}(0)\,|\pi^b(q)\rangle$, we find (see [7])

$$\langle 0|\, j^{\mu 5a}(0)\,|\pi^b(q)\rangle = i f \delta^{ab} q^\mu. \tag{1.67}$$

Comparing with (1.63), we find $f = f_\pi$, which has been measured to be $f_\pi = 93$ MeV.

In eqn. (1.41) we had the electroweak scale v instead of f_π, but this is the only difference between the effective Lagrangian we found for chiral symmetry breaking in QCD and the non-gauged version of the SM Higgs sector! We could now indeed take the weak interactions into acoount and gauge the $SU(2)_L \otimes U(1)_Y$ subgroup of $SU(2)_L \otimes SU(2)_R$ exactly like we did in section 1.2. QCD would thus *dynamically* (by the formation of a quark anti-quark condensate) break the $SU(2)_L \otimes U(1)_Y$ gauge symmetry of the electroweak sector.

We note that just the following two problems prevent us from using QCD to get the desired symmetry breaking pattern in the Standard Model instead of the SM Higgs sector[6]:

1. The scale $f_\pi = 93$ MeV is 2600 times too small compared to $v = 246$ GeV,

2. We observe the QCD pion degrees of freedom in the spectrum, they thus cannot give the weak gauge bosons mass.

This is the motivation to postulate a new strong (QCD-like) interaction with $f = 246$ GeV, called *Technicolor.*

[6]There are of course more subtleties involved here. For example, the SM also needs the Higgs particle to unitarize the W scattering. We here just want to illustrate a point.

1.4 Technicolor

In the last section we saw that the Higgs sector in the SM induces exactly the same symmetry breaking structure as the effective linear sigma model we wrote to model the spontaneous breaking of chiral symmetry in QCD, except that the pion decay constant is roughly 2600 times too small. Spontaneous symmetry breaking in QCD is due to the formation of a chiral condensate and thus evolves dynamically without having to introduce an elementary scalar to break the symmetry.

Since elementary scalars are problematic[7], an electroweak symmetry breaking process like in QCD would be desirable. Furthermore, this would provide a dyamical explanation *why* there is a symmetry breaking, which the SM lacks. If we take QCD as a prototype for dynamical symmetry (DSB) with a composite order parameter, we are thus naturally led to introduce a new scaled up QCD-like interaction, which is called Technicolor (TC).

To make things a little more concrete, we will now introduce the simplest TC model, which was first introduced by Susskind and Weinberg. As in every Technicolor model we have to enlarge the gauge symmetry structure of the SM by the Technicolor group $SU(N_T)$. This means that we have to introduce $N_T^2 - 1$ additional gauge bosons, called Technigluons. The whole gauge symmetry structure is thus $SU(N_T) \otimes SU(3)_{\text{QCD}} \otimes SU(2)_L \otimes U(1)_Y$.

Furthermore we need to include at least one flavor doublet of techniquarks, which are charged under $SU(N_T)$ and thus carry the index[8] $a = 1, \ldots, N_T$: $(U,\ D)^a$. We will consider them to be exactly massless and analogous to what we did in QCD thus have independent left- and right-handed parts to which we assign the following quantum numbers

[7]This is mostly connected to the quadratic divergent mass corrections of scalars, but also due to the fact that so far there have not been seen any fundamental scalars in nature. See ref. [11].

[8]In this simplest model we choose not to give the techniquarks a charge under the $SU(3)$, which would give rise to another index. See [11] for generalizations.

under the gauge symmetry group from above:

$$\begin{aligned} \begin{pmatrix} U \\ D \end{pmatrix}_L^a &\sim (N,\ 1,\ 2,\ 0) \\ U_R &\sim (N,\ 1,\ 1,\ 1/2) \\ D_R &\sim (N,\ 1,\ 1,\ -1/2)\,. \end{aligned} \tag{1.68}$$

The right-handed fields are singlets under $SU(2)_L$. Ignoring again the $U(1)$ groups which are not spontaneously broken (see [11]), the global chiral symmetry group is just $SU(2)_L \otimes SU(2)_R$, if we include only one chiral doublet of techniquarks.

If we replace $q = (u, d)$ in the last section by $Q = (U, D)$ and also replace the pion decay constant $f_\pi = 93$ MeV by the up-scaled technipion decay constant $F_{TC} \approx 250$ GeV and again use the linear sigma model, we exactly reproduce the symmetry breaking structure of the SM Higgs sector, but now with a composite and not an elementary "Higgs" field.[9] The Nambu-Goldstone bosons (NGB) are (just as in the case of an elementary Higgs) eaten by the gauge bosons to give them masses. So there are no NGB left in the spectrum. This would change, if we had introduced more than one doublet of techniquarks, see [11].

Scaling Up QCD

Let $\Lambda_{\rm QCD}$ by the scale of QCD, meaning the scale where the QCD interactions become strong, i.e. at $\alpha_S(\Lambda_S) \approx 1$. In analogy let $\Lambda_{\rm TC}$ be the TC scale. We already introduced the two decay constants f_π and $F_{\rm TC}$ and the electroweak scale $v = 246$ GeV. Continuing to consider the case with only one techniquark doublet we can write down the following scaling rules (see [11] for a more detailed treatment):

$$F_{\rm TC} \approx v, \quad \frac{\Lambda_{\rm TC}}{\Lambda_{\rm QCD}} = \frac{v}{f_\pi} \frac{\sqrt{3}}{\sqrt{N_T}}. \tag{1.69}$$

Using $\lambda_{QCD} \approx 200$ MeV, $f_\pi \approx 93$ MeV and assuming $N_T = 4$, we thereby estimate $\Lambda \approx 460$ GeV. This is assumed to be the scale where we have hadronization of techniquarks due

[9] It is important to note that this particle just plays the same role as the SM Higgs in the sense that it acquires a non zero vev and thus drives the symmetry breaking. The coupling of this particle is unknown and not proportional to the mass of the particle it is coupling to like the SM Higgs.

to $\alpha_{\mathrm{TC}} \approx 1$. Depending on the Technicolor model one assumes, there is a rich spectrum of technihadrons (technimesons consisting of linear combinations of quark anti-quark states and technibaryons consisting of N_T techniquarks) forming at that scale. For a detailed discussion of the experimental implications of this see ref. [11].

Although we can write down a low energy effective theory of TC which resembles the Higgs sector of the SM, we should emphasize here that TC does not necessarily *need* a Higgs boson. We could well use the non-linear sigma model to model the chiral symmetry breaking and just have the pion degrees of freedom.

Let us now look at what mass scale we expect to find the mass of the lightest vector meson, the techni-ρ. Looking at the QCD analogue, the ρ meson, we find in the case of having one flavor techniquark doublet (see ref. [11]):

$$m_{\rho\mathrm{TC}} \approx m_\rho \frac{v}{f_\pi} \sqrt{\frac{3}{N_T}}. \tag{1.70}$$

Using again the values from above and $m_\rho = 770\,\mathrm{MeV}$, we find $m_{\rho\mathrm{TC}} \approx 1.8\,\mathrm{TeV}$.

The TC model we have considered so far is incomplete because of two major aspects: At first, we so far did not explain how the masses of the fermions are generated. Secondly, we have many heavy technihadron states which are stable and we would like to provide a mechanism which let this states decay to ordinary hadrons. We will therefore introduce Extended Technicolor in the next section.

1.5 Extended Technicolor

To provide for a possible decay channel of technihadrons into ordinary hadrons we introduce a model with another interaction which couples technifermions to Standard Model fermions: Extended Technicolor (ETC). We will see that this new interaction is also able to generate masses for the Standard Model fermions.

We will here mostly follow [3] and present just the general ETC idea, which is independent of details which vary between different ETC models and are reviewed in ref. [11].

Note that the mass generation process of ETC is analogous to what we will discuss in section 2.1 for the top mass generation of Topcolor models. We will therefore not discuss details of this process here.

Let us introduce the so called master gauge group G_{ETC}, which enlarges the Technicolor group by placing the Technicolor fermions together with the ordinary fermions in one irreducible representation of G_{ETC}. The master gauge group is supposed to break down to Technicolor at the scale μ (due to some process which we leave unspecified here). The gauge bosons of Extended Technicolor couple to both, ordinary fermions f and technifermions F, whereas the gauge bosons of TC[10]only couple to the technifermions. Moreover, there will be gauge bosons $\mathcal{E}$ which are in ETC, but not in TC. The following diagram illustrates this:

$$(F \quad F \quad F \quad f)$$
$$\longleftrightarrow \quad \text{TC}$$
$$\longleftrightarrow \quad \text{ETC}$$

Due to the symmetry breaking, the gauge bosons $\mathcal{E}$ acquire the mass[11] $M_{\mathcal{E}} \approx g_{\mathrm{ETC}}\mu$, where g_{ETC} is the coupling constant of ETC. This gauge boson couples to currents of the form $\bar{F}_L \gamma_\mu f$, as illustrated in Fig. 1.2.

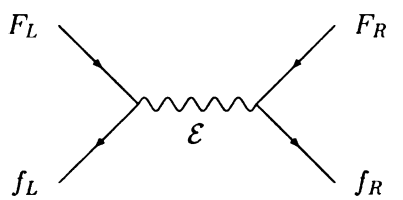

Figure 1.2. ETC interaction between ordinary fermions and technifermions.

The corresponding four fermion interaction has the form

$$\frac{1}{2}\left(\frac{g_{\mathrm{ETC}}}{M_{\mathcal{E}}}\right)^2 \left(\bar{F}_L \gamma_\mu f_L\right)\left(\bar{f}_R \gamma^\mu F_R\right). \tag{1.71}$$

[10] The TC gauge bosons must be a linear combination of some ETC gauge bosons, since TC is assumed to be an unbroken subgroup of ETC.

[11] This is just an estimate, but we will see that this is the general form of the gauge boson mass terms for an explicit example in section 2.3.

After doing a Fierz transformation we see that this interaction contains the following term:

$$-\frac{1}{2\mu^2}\left(\bar{F}F\right)\left(\bar{f}f\right).$$

If now (at a much lower scale than μ) the Technicolor condensate forms, we can put $\bar{F}F$ into its vev $\langle\bar{F}F\rangle$ and get a mass term for the fermion f:

$$m_f = \frac{1}{2\mu^2}\langle\bar{F}F\rangle, \tag{1.72}$$

where we also used $M_{\mathcal{E}} \approx g_{\mathrm{ETC}}\mu$. We can now estimate $\langle\bar{F}F\rangle$ with the scale of Technicolor:[12] $\langle\bar{F}F\rangle \sim (1\ \mathrm{TeV})^3$.

We thus need high scales μ to produce small fermion masses. For example we need $\mu \approx 30$ TeV to produce $m_f \approx 1$ GeV.

As we will see explicitly in section 3.1 for the Topcolor model we are going to introduce, the general ETC interactions will also give rise to flavor changing neutral currents (FCNC), induced by (four-fermion interaction) terms like:

$$\frac{1}{\mu^2}\left(\bar{s}_L\gamma_\mu d_L\right)\left(\bar{d}_R\gamma^\mu s_R\right). \tag{1.73}$$

Now one of the big problems of ETC is the following: The large top mass would force μ to be rather small (see eqn. (1.72)) and the FCNC like in (1.73) would then not be suppressed enough to fulfill the tight experimental bounds on FCNC. See [11] for details.

This inability to produce a heavy top quark is the motivation to introduce Topcolor assisted Technicolor models [10] in which the large top mass arises due to another interaction. We introduce Topcolor assisted Technicolor in the next chapter.

[12] This is commonly done. However, we will calculate such a vev in the Nambu-Jona-Lasinio model in section 2.1.

Chapter 2

Introducing the Modified Topcolor Model

2.1 The Topcolor Idea in the Nambu-Jona-Lasinio Approximation

We will in this thesis be interested in a modification of a Topcolor assisted Technicolor model which was introduced by Simmons and Popovic [14]. But before we introduce this model and its gauge groups, we would like to motivate the general form of Topcolor models like this one.

Our first goal is to introduce a new interaction, called *Topcolor* [9], which dynamically gives a mass to the top quark[1] similar to the mass generation process in ETC.
Analogous to ETC, if we could find a gauge interaction which, after Fierz rearrangement, contains the following term

$$\frac{8\pi\kappa}{M^2}\left(\bar{\psi}_L t_R\right)\left(\bar{t}_R \psi_L\right), \tag{2.1}$$

then we could provide a large top mass, if this interaction became strong at a certain scale and would form a condensate $\langle \bar{t}_L t_R \rangle \neq 0$. Note that ψ_L denotes the top-bottom chiral doublet and that we have put in the factor 8π for later convenience. Further note that just like the TC condensate, $\langle \bar{t}_L t_R \rangle \neq 0$ breaks the electroweak symmetry as we will see in section 2.5. Also motivated by the fact that the top quark mass is comparable to the electroweak scale v, early Topcolor models [9] therefore suggested that the whole electroweak symmetry breaking is due to a top quark condensate, without introducing TC. But it turned

[1] We will assume that the other fermion masses can be produced via ETC.

out that these models predict a much too large top mass, see ref. [11].

Using a Fierz transformation, one can show (see ref. [11])

$$-\frac{8\pi\kappa}{M^2}\left(\bar{\psi}_L\gamma_\mu\frac{\lambda^A}{2}\psi_L\right)\left(\bar{t}_R\gamma^\mu\frac{\lambda^A}{2}t_R\right)=\frac{8\pi\kappa}{M^2}\left(\bar{\psi}_L t_R\right)\left(\bar{t}_R\psi_L\right)+\ldots, \tag{2.2}$$

with the $SU(3)$ generating Gell-Mann matrices λ^A. Thus we infer the gauge structure of our Topcolor interaction to be $SU(3)$. Since we want the gauge boson to acquire the mass M, the gauge group which we introduce has to be spontaneously broken at some scale. On the other hand, we know that at low energies we have to produce the unbroken $SU(3)_C$ group of QCD. We can do so by introducing the gauge group structure $SU(3)_1 \otimes SU(3)_2$ which gets spontaneously broken down to $SU(3)_C$ due to some process which we leave unspecified here.

Furthermore, we assume that one group, let us say the first one, becomes strong at an energy at the TeV scale[2] and that only the third generation quarks transform under this strong group, whereas the others transform under the weaker $SU(3)_2$ group.

Using the Nambu-Jona-Lasino (NJL) toy model of chiral symmetry breaking, we will in the following show, how a top quark condensation could then give mass to the top quark.

In the NJL model one assumes a Lagrangian of the form

$$\mathcal{L}_{\text{NJL}}=\bar{\psi}_L i\partial\!\!\!/\psi_L+\bar{\psi}_R i\partial\!\!\!/\psi_R+\frac{8\pi\kappa}{M^2}\left(\bar{\psi}_L t_R\right)\left(\bar{t}_R\psi_L\right), \tag{2.3}$$

where we recognize the last term to be the left-hand side of eqn. (2.2). The approximation we are making in assuming this Lagrangian to describe our simple Topcolor model lies in ignoring the interactions in the ellipses of eqn. (2.2). Before we begin the calculation, let us illustrate the process of the top[3] mass generation graphically.

The Topcolor interaction induces interactions between left- and right-handed top quarks via the exchange of topgluons (sometimes also called Colorons). After the interaction

[2]Analogous to QCD, which becomes strong at $\Lambda_{\text{QCD}} \approx 200$ MeV.

[3]Actually, this simple version of Topcolor is not able to distinguish between the top and bottom quark and thus would in the same way generate an unwanted mass for the bottom quark. We will take that into account later.

becomes strong, we will see that under certain circumstances there will be a top condensate to which the top quark couples when moving through the vacuum:

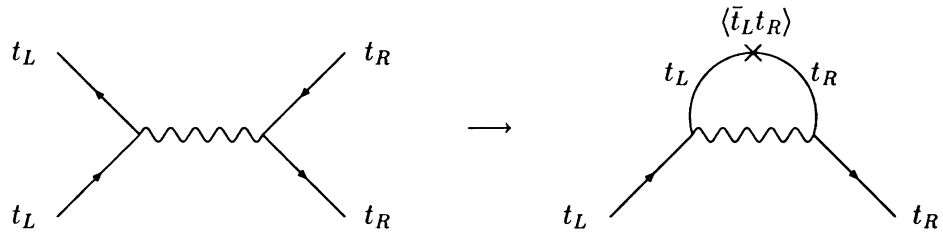

At low energies this gives rise to the diagram shown at the right-hand side of Fig. 2.1. This diagram has the right form to be identified with a dynamical mass term[4].

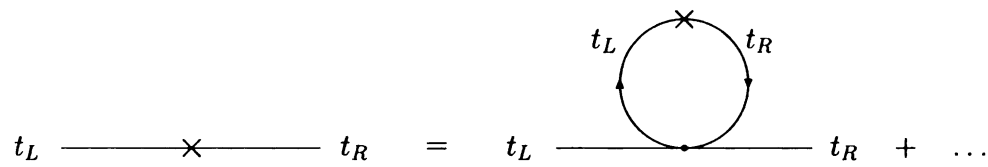

Figure 2.1. Dynamical top mass generation.

We now make the following self-consistent ansatz: *If* the top quark gets a dynamical mass m, then (in the NJL approximation) it must be due to diagrams like the one shown in Fig. 2.1. Using the Feynman rules we thus translate the diagrams of Fig. 2.1 into the following equation[5]:

$$\begin{aligned} -im &= -iN_C \frac{8\pi\kappa}{M^2} \int \frac{d^4k}{(2\pi)^4} \operatorname{Tr}\left[\frac{i\,(\not{k}+m)}{k^2-m^2}\frac{1}{2}\,(1+\gamma_5)\right] \\ &= N_C \frac{8\pi\kappa}{M^2} \int \frac{d^4k}{(2\pi)^4} 4 \frac{m}{k^2+m^2}\frac{1}{2} \\ &= N_C \frac{16\pi\kappa}{M^2} i \int \frac{d^4k_E}{(2\pi)^4} \frac{m}{-k_E^2-m^2}, \end{aligned}$$

where N_C is the color factor and we used $\operatorname{Tr}\gamma_5 = 0, \operatorname{Tr}\mathbb{1}m = 4m$ and that the term proportional to $\not{k}$ vanishes due to the anti-symmetry to get the second line. In the third line

[4]Fermion mass terms are proportional to $\bar{\psi}\psi = \bar{\psi}_L\psi_R + \bar{\psi}_R\psi_L$.

[5]Thanks to Prof. Chivukula and Prof. Simmons for helping me doing this calculation.

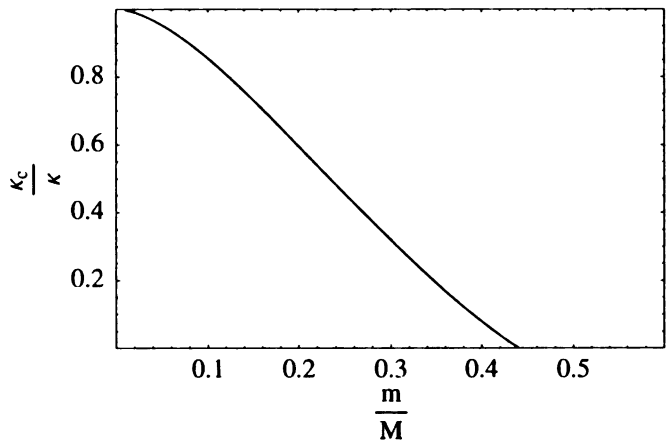

Figure 2.2. Illustration of the solution to the gap equation.

we went to Euclidean space, $k^0 = ik_E$. We now use $d^4k_E = \pi^2 k_E^2 dk_E^2$ to get

$$m = \frac{N_C \kappa}{\pi M^2} m \int dk_E^2 \frac{k_E^2}{k_E^2 + m^2}. \tag{2.4}$$

This intergral is ultra-violet divergent. The reason for that is our four-fermion approximation which is no longer valid if $k^2 \sim M^2$. We thus use the cut-off M^2 and solve the integral to get:

$$m = \frac{N_C \kappa}{\pi M^2} m \left[M^2 - m^2 \ln \frac{M^2}{m^2} \right], \tag{2.5}$$

which is called the *gap equation*. The case $m = 0$ is trivial and belongs to the case where no symmetry breaking occured. In the case $m \neq 0$, we can rewrite our result:

$$\frac{N_C}{\pi} - \frac{1}{\kappa} = \frac{m^2}{M^2} \ln \frac{M^2}{m^2}. \tag{2.6}$$

We now define the critical coupling $\kappa_c \equiv \pi / N_C$ and see that this equation does not have a solution for $\kappa < \kappa_c$. In this case we do not get a dynamical mass and $\langle \bar{t}_L t_R \rangle = 0$ must hold. Thus the system is in the Wigner phase (see section 1.1). If then the coupling gets stronger, $\kappa > \kappa_c$ we have $m \neq 0$ and $\langle \bar{t}_L t_R \rangle \neq 0$. We thus have a *phase transition* to the Nambu-Goldstone phase.

Fig. 2.2 illustrates solutions from the gap equation. We see that if the gauge boson mass is very large compared to the top mass, we are forced to κ being very close to its critical

value κ_c.

In the Topcolor model which we will introduce in the next section, we do not want the bottom quark to also form a condensate, so we must provide for another interaction which distinguishes between the bottom and the top quark. This will complicate the critical conditions for condensation, but we will still find that large gauge boson masses (compared to the top mass) force us to regions very near the critical region.

We will later also need another result which can be derived in the NJL model approximation: The so called *Pagels-Stokar relation* connects the scale Λ where an interaction becomes strong (in our case this will be the Topcolor scale), to the pion decay constant f and the dynamical mass m (in our case the top mass) generated by the formation of the condensate:

$$f^2 = \frac{3m^2}{8\pi^2} \ln \frac{\Lambda^2}{m^2}, \tag{2.7}$$

in the limit $m \ll \Lambda$. See the appendix of ref. [11] for a derivation.

2.2 The Model and its Gauge Groups

Similar to the models proposed by Simmons and Popovic [14] and Hill [10], we would like to introduce a Topcolor assisted Technicolor model, i.e. we assume that all particles, except the top quark get their masses from ETC. The mass contribution from ETC to the top quark is assumed to be of the order of the bottom quark, or smaller.

As motivated in the last section, we will assume a $SU(3)_1 \otimes SU(3)_2$ Coloron sector with the third generation quarks transforming under the stronger $SU(3)_1$ group, which breakes down to the SM QCD group $SU(3)_C$ at the scale u of order a few TeV.

We will also introduce another interaction, which distinguishes between the top and bottom quark to be able to produce a top condensate without having a bottom quark or any other condensate (see section 2.6 for a discussion of the resulting critical couplings). In order to be able to reproduce the SM $U(1)_Y$ hypercharge group, we introduce the gauge

	$SU(N)_{TC}$	$SU(3)_1$	$SU(3)_2$	$SU(2)_W$	$U(1)_1$	$U(1)_2$
I	1	1	SM	SM	SM	0
II	1	1	SM	SM	SM	0
III	1	SM	1	SM	SM	0

Table 2.1. Gauge charge assignments for fermions of I, II and III generation. "SM" indicates assignment corresponding to the Standard Model.

groups $U(1)_1 \otimes U(1)_2$ which are assumed to be spontaneously broken to $U(1)_Y$ also at the scale u. We will not specify the symmetry breaking at the scale u further and just assume some (maybe composite) scalar Φ acquiring a non-zero vev at that scale. We will discuss this symmetry breaking in section 2.3.

The whole gauge group structure is thus

$$SU(N)_{TC} \otimes SU(3)_1 \otimes SU(3)_2 \otimes SU(2)_W \otimes U(1)_1 \otimes U(1)_2. \tag{2.8}$$

Table 2.1 shows the fermion charge assignments of our model, which has a flavor-universal hypercharge sector, but treats the third generation differently in the Coloron sector. This is what makes this Topcolor model different from the Simmons and Popovic [14] Topcolor model, which treates the third generation differently in the *hypercharge* sector. See chapter 4.

The electroweak symmetry breaking down to the QED gauge group $U(1)_{\text{em}}$ is a little more complicated and will be partly driven by a top condensate and partly by a Technicolor condensate and we discuss it in section 2.5. We can summarize the different symmetry breaking by the following diagram (leaving aside the TC and ETC gauge groups):

$$\begin{array}{c} SU(3)_1 \otimes SU(3)_2 \otimes SU(2)_L \otimes U(1)_1 \otimes U(1)_2 \\ \downarrow u \\ SU(3)_C \otimes SU(2)_L \otimes U(1)_Y \\ \downarrow v \\ SU(3)_C \otimes U(1)_{\text{em}}. \end{array}$$

2.3 The First Symmetry Breaking at the TeV Scale

Let us assign the coupling constants $g_{\rm TC}$, h_1, h_2, g, g_1' and g_2' to our gauge groups

$$SU(N)_{TC} \otimes SU(3)_1 \otimes SU(3)_2 \otimes SU(2)_W \otimes U(1)_1 \otimes U(1)_2. \tag{2.9}$$

Furthermore we introduce a scalar $\Phi_\alpha^{\beta 6}$ transforming as $\left(1, 3, \bar{3}, 1, p/2\sqrt{6}, -p/2\sqrt{6}\right)$, where p is some real (positive) number and the factor of $1/2\sqrt{6}$ will turn out to be convenient. Note that we allow p to be an additional degree of freedom in our theory. But since it is associated with a hypercharge, we expect it to be of order one.

In order to break $SU(3)_1 \otimes SU(3)_2$ and $U(1)_1 \otimes U(1)_2$ at the scale u down to their diagonal subgroups $SU(3)_C$ and $U(1)_Y$, respectively, we assume that the scalar Φ acquires the following non-zero vev

$$\langle \Phi_\alpha^\beta \rangle = u\, \delta_\alpha^\beta. \tag{2.10}$$

The covariant derivative, to be applied to Φ, then looks like[7]

$$D_\mu = \partial_\mu \mathbb{1} + i h_1 A_{1\mu}^A T_1^A + i h_2 A_{2\mu}^A T_2^A + i g_1' B_{1\mu} Y_1 \mathbb{1} + i g_2' B_{2\mu} Y_2 \mathbb{1}. \tag{2.11}$$

We will suppress unit matrices like those in (2.11) from now on, for the sake of a more readable notation. In the fundamental 3 representation we may write $T_1^A = \frac{\lambda^A}{2}$, and, likewise, $T_2^A = -\left(\frac{\lambda^A}{2}\right)^T$ in the conjugate $\bar{3}$ representation, where λ^A are the eight Gell-Mann matrices. To find the mass matrix for the gauge bosons, we use equation (B.4) and apply the covariant derivative to the vacuum expectation value of Φ, equation (2.10):

$$\left(D_\mu \langle \Phi \rangle\right)_\alpha^\beta = i\frac{u}{2}\left(\lambda^A\right)_\alpha^\beta \left(h_1 A_{1\mu}^A - h_2 A_{2\mu}^A\right) - iu\frac{p}{2\sqrt{6}}\delta_\alpha^\beta\left(g_1' B_{1\mu} - g_2' B_{2\mu}\right). \tag{2.12}$$

Now using that the Gell-Mann matrices are traceless, that $\delta_\alpha^\beta \delta_\beta^\alpha = 3$ and the following relation for the Gell-Mann matrices

$$\left(\lambda^A\right)_\alpha^\beta \left(\lambda^B\right)_\beta^\alpha = 2\delta^{AB}, \tag{2.13}$$

[6]See section B in the appendix for an explanation of the conjugate representation and the index notation we use.

[7]We use the convention $Q = T_3 + Y$.

one finds for the kinetic part of Φ,

$$\begin{aligned}
&\left(D_\mu\langle\Phi\rangle\right)^{\dagger\beta}_{\alpha}\left(D_\mu\langle\Phi\rangle\right)_{\beta}{}^{\alpha} \\
&= \frac{u^2}{4}\left[(\lambda^A)^\beta_\alpha(\lambda^B)^\alpha_\beta\left(h_1A^A_{1\mu}-h_2A^A_{2\mu}\right)\left(h_1A^B_{1\mu}-h_2A^B_{2\mu}\right)\right] \\
&\quad + u^2\frac{p^2}{24}\delta^\beta_\alpha\delta^\alpha_\beta\left(g'_1B_{1\mu}-g'_2B_{2\mu}\right)\left(g'_1B^\mu_1-g'_2B^\mu_2\right) \\
&= \frac{u^2}{2}\Big[h_1^2A^A_{1\mu}A^{A\mu}_1-2h_1h_2A^A_{1\mu}A^{A\mu}_2+h_2^2A^A_{2\mu}A^{A\mu}_2 \\
&\quad + \frac{p^2}{4}\left(g_1'^2B_{1\mu}B^\mu_1-2g'_1g'_2B_{1\mu}B^\mu_2+g_2'^2B_{1\mu}B^\mu_1B_{2\mu}B^\mu_2\right)\Big].
\end{aligned}$$

The right hand side can be put into matrix form:

$$\frac{u^2}{2}\begin{pmatrix}A^A_{1\mu}\\A^A_{2\mu}\\B_{1\mu}\\B_{2\mu}\end{pmatrix}^T\begin{pmatrix}h_1^2 & -h_1h_2 & 0 & 0\\ -h_1h_2 & h_2^2 & 0 & 0\\ 0 & 0 & \frac{p^2}{4}g_1'^2 & -\frac{p^2}{4}g'_1g'_2\\ 0 & 0 & -\frac{p^2}{4}g'_1g'_2 & \frac{p^2}{4}g_2'^2\end{pmatrix}\begin{pmatrix}A^{A\mu}_1\\A^{A\mu}_2\\B^\mu_1\\B^\mu_2\end{pmatrix}. \tag{2.14}$$

Now the mass matrix of the gauge bosons (2.14) can be rotated to its mass eigenstate basis by diagonalizing it. Defining $\cos\beta \equiv h_1/\sqrt{h_1^2+h_2^2}$ and $\sin\beta \equiv h_2/\sqrt{h_1^2+h_2^2}$, we obtain for the mass eigenstates C^A_μ (massive Coloron fields) and G^A_μ (massless gluon fields of QCD), the relations

$$\begin{aligned}
C^A_\mu &= \cos\beta\, A^A_{1\mu} - \sin\beta\, A^A_{2\mu},\\
G^A_\mu &= \sin\beta\, A^A_{1\mu} + \cos\beta\, A^A_{2\mu}.
\end{aligned} \tag{2.15}$$

An analogous transformation can be made for the $U(1)$ fields, where the Standard Model hypercharge field remains massless and the field orthogonal to that, which we denote Z' hereafter, acquires a mass. By applying these transformations to (2.14), one finds for the two massive fields

$$\begin{aligned}
M_C &= u\sqrt{h_1^2+h_2^2},\\
M_{Z'} &= u\,\tfrac{p}{2}\sqrt{g_1'^2+g_2'^2}.
\end{aligned} \tag{2.16}$$

Since we will be working in the electroweak sector most of the time, we also define

$$u' \equiv p\,u \tag{2.17}$$

for later simplification of the notation. Then

$$\begin{aligned} M_C &= \frac{u'}{p}\sqrt{h_1^2 + h_2^2} \\ \text{and } M_{Z'} &= \frac{u'}{2}\sqrt{g_1'^2 + g_2'^2}. \end{aligned} \tag{2.18}$$

The gluon and hypercharge fields of the Standard Model (before electroweak symmetry breaking) are orthogonal to the massive Coloron and Z' fields and therefore remain massless.

2.4 The Effective Lagrangian

Using the charges of table 2.1, replacing the derivative in the fermion kinetic energy terms by the covariant derivative and plugging in the mass eigenstates from eqn. (2.15), yields

$$\bar{f}_{I,II} i\not{D} f_{I,II} + \bar{f}_{III} i\not{D} f_{III} = \ldots - C_\mu^A J_C^{A\mu} - G_\mu^A J_G^{A\mu}, \tag{2.19}$$

where f denotes any fermion and the currents are defined by

$$J_C^{A\mu} \equiv h_1 \cos\beta \bar{f}_{III}\gamma^\mu \tfrac{\lambda^A}{2} f_{III} - h_2 \sin\beta \bar{f}_{I,II}\gamma^\mu \tfrac{\lambda^A}{2} f_{I,II} \tag{2.20}$$

$$\text{and } J_G^{A\mu} \equiv h_1 \sin\beta \bar{f}_{III}\gamma^\mu \tfrac{\lambda^A}{2} f_{III} + h_2 \cos\beta \bar{f}_{I,II}\gamma^\mu \tfrac{\lambda^A}{2} f_{I,II}. \tag{2.21}$$

We now define $g' \equiv g_1' g_2'/\sqrt{g_1'^2 + g_2'^2}$ and $g_S \equiv h_1 h_2/\sqrt{h_1^2 + h_2^2}$, which will soon be recognized to be the $U(1)_Y$ and $SU(3)_C$ coupling constants of the unbroken subgroups. We further define $\alpha_Y \equiv g'^2/4\pi$, $\alpha_S \equiv g_S^2/4\pi$ and

$$\kappa_1 \equiv \alpha_Y \left(\frac{g_1'}{g_2'}\right)^2, \quad \kappa_3 \equiv \alpha_S \left(\frac{h_1}{h_2}\right)^2. \tag{2.22}$$

Then eqns. (2.20) and (2.21) can be rewritten

$$J_C^{A\mu} = \sqrt{4\pi}\left(\sqrt{\kappa_3}\bar{f}_{III}\gamma^\mu \tfrac{\lambda^A}{2} f_{III} - \frac{\alpha_S}{\sqrt{\kappa_3}} \bar{f}_{I,II}\gamma^\mu \tfrac{\lambda^A}{2} f_{I,II}\right) \tag{2.23}$$

$$J_G^{A\mu} = g_3\left(\bar{f}\gamma^\mu \tfrac{\lambda^A}{2} f\right), \tag{2.24}$$

where we used $\kappa_3 = \frac{1}{4\pi}\cos^2\beta\, h_1^2$. For low energies, meaning $p^2 \ll M_C^2$ and $p^2 \ll M_{Z'}^2$, this yields the effective Lagrangian

$$\begin{aligned}\mathcal{L}_C &= -\frac{1}{2M_C^2} J_{C\mu}^A J_C^{A\mu} \\ &= -\frac{2\pi}{M_C^2}\left(\sqrt{\kappa_3}\bar{f}_{III}\gamma_\mu\frac{\lambda^A}{2}f_{III} - \frac{\alpha_S}{\sqrt{\kappa_3}}\bar{f}_{I,II}\gamma_\mu\frac{\lambda^A}{2}f_{I,II}\right)^2,\end{aligned} \tag{2.25}$$

where the factor of two in the denominator comes from the symmetry factor in the Feynman Rules for two identical currents. Correspondingly the result for the hypercharge fields is

$$\mathcal{L}_{Z'} = -\frac{2\pi}{M_{Z'}^2}\kappa_1\left(\bar{q}\gamma^\mu Y q\right)^2, \tag{2.26}$$

where q denotes any quark.

So far (without having taken into account the electroweak symmetry breaking yet) our theory has four independent parameters, which we will choose to be κ_1, κ_3, p and the scale u or u' to be consistent with [14]. We should therefore re-express the results for the Coloron and the Z' masses in terms of these parameters. For that purpose we first recall:

$$\begin{aligned}\alpha_Y &= \frac{1}{4\pi}\frac{g_1'^2 g_2'^2}{g_1'^2 + g_2'^2} \\ \kappa_1 &= \alpha_Y\frac{g_1'^2}{g_2'^2} = \frac{1}{4\pi}\frac{g_1'^4}{g_1'^2 + g_2'^2}.\end{aligned}$$

So we get

$$\begin{aligned}\frac{\kappa_1}{\alpha_Y} &= \frac{g_1'^2}{g_2'^2} \quad \text{and} \\ \frac{1}{g_1'^2} &= \frac{1}{4\pi\alpha_Y} - \frac{1}{g_2'^2}.\end{aligned}$$

We can solve this to find:

$$g_1'^2 = 4\pi\left(\kappa_1 + \alpha_Y\right), \tag{2.27}$$

$$g_2'^2 = 4\pi\frac{\alpha_Y}{\kappa_1}\left(\kappa_1 + \alpha_Y\right). \tag{2.28}$$

We can do the same for the Coloron sector and get:

$$h_1^2 = 4\pi\left(\kappa_3 + \alpha_S\right), \tag{2.29}$$

$$h_2^2 = 4\pi\frac{\alpha_S}{\kappa_3}\left(\kappa_3 + \alpha_S\right). \tag{2.30}$$

Now we can rewrite the Coloron and Z' mass, eqns. (2.18), in terms of κ_1, κ_3, p and u':

$$\begin{aligned} M_C &= \frac{u'}{p}\sqrt{\frac{4\pi}{\kappa_3}}\left(\kappa_3 + \alpha_S\right), \\ M_{Z'} &= u'\sqrt{\frac{\pi}{\kappa_1}}\left(\kappa_1 + \alpha_Y\right). \end{aligned} \tag{2.31}$$

2.5 Electroweak Symmetry Breaking

In section 2.3 we only took into account the first part of the symmetry breaking. The complete pattern of the breaking, including the corresponding gauge boson fields, is:

$$\begin{array}{c} \overset{W^{a\mu}}{SU(2)_L} \otimes \overset{B_1^\mu}{U(1)_1} \otimes \overset{B_2^\mu}{U(1)_2} \\ \downarrow\ u \\ \overset{W^{a\mu}}{SU(2)_L} \otimes \overset{Z'^\mu_\perp}{U(1)_Y} \\ \downarrow\ v \\ \overset{A^\mu}{U(1)_{em}}. \end{array}$$

In this section we will see that the Z boson field coupling of our model is not the same as in the Standard Model, but will be slightly shifted. Except that we will explicitly use the sigma model to derive the mass matrix, we will in this section follow ref. [4].

Fig. 2.3 illustrates the whole symmetry breaking structure in the electroweak sector in a moose diagram. As denoted in Fig. 2.3, we introduce a complex scalar field σ to break the $U(1)$-groups down to their diagonal subgroups at the scale u. The electroweak symmetry breaking is realized partially by the top-condensates and partially by the Technicolor-condensates as will be discussed in detail.

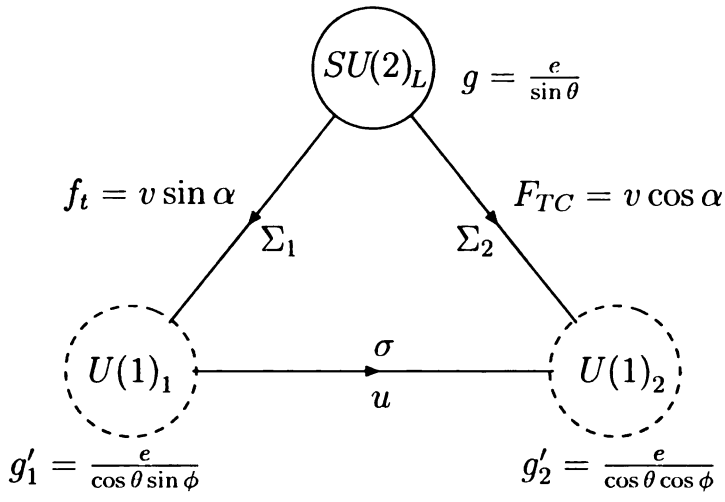

Figure 2.3. The pattern of the symmetry breaking of the electroweak sector in moose notation.

It is now worthwile to pause for a minute and to think about the number of independent parameters we have. We have three symmetry breaking scales u, f_t, F_{TC} and from experiment we know the electroweak scale to be $v^2 = 1/\sqrt{2}G_F$ derived from the extremely well measured Fermi constant G_F. The Technicolor and the Topcolor scale have to reproduce this overall scale:

$$F_{TC}^2 + f_t^2 = v^2. \tag{2.32}$$

Thus we are only free to choose two scales independently, e.g. u and f_t. We also know the $SU(2)$ coupling constant g to be $g = e/\sin\theta$ (see section 2.10 for a discussion of how to relate $\sin\theta$ to observables). In the same sense we know the coupling of the Standard Model hypercharge group $g' = e/\cos\theta$. As we discussed in section 2.4, $g' = g'_1 g'_2/\sqrt{{g'_1}^2 + {g'_2}^2}$. This yields only one additional degree of freedom for the choice of the coupling constants (g'_1, g'_2) of the two $U(1)$ groups.

Finally, as in section 2.3, we will have one additional degree of freedom, denoted p, associated with the $U(1)_1$ and $U(1)_2$ charges of the scalar σ which drives the symmetry breaking at the scale u. We will see that p always appears multiplied by u, so we will absorb it in our definition of $u' = up$.

Altogether we therefore have four degrees of freedom which we could choose to be κ_1, p, u, f_t. Instead we will find it more convenient to exchange f_t and κ_1 for the two new parameters

$$\sin\alpha = \frac{f_t}{v} \quad \text{and} \tag{2.33}$$

$$\sin^2\phi = \frac{g_2'^2}{g_1'^2 + g_2'^2} = \frac{\alpha_Y}{\kappa_1 + \alpha_Y}, \tag{2.34}$$

where the angle ϕ can readily be recognized to be the mixing angle rotating the gauge eigenstates of the $U(1)$ gauge bosons into their mass eigenstates.

To realize the electroweak symmetry breaking via the Technicolor and Topcolor condensates, we will use the non-linear sigma model introduced in section 1.2. We therefore define the following two Σ-fields parameterized by the Topcolor and Technicolor pions:

$$\Sigma_1 = e^{i\tau^a \pi_1^a(x)/f_t} \quad \text{and} \quad \Sigma_2 = e^{i\tau^a \pi_2^a(x)/F_{TC}}, \tag{2.35}$$

where we introduced $\tau^a \equiv \frac{\sigma^a}{2}$ with the Pauli matrices σ^a. When we now define the transformation properties of the Sigma fields, we have to take into account that the $U(1)$ gauge groups form abelian subgroups of a global $SU(2)_R$. We can take the T^3-operator (with the diagonal representation τ^3) to generate it (as we did in chapter 1.2). The transformations then look like

$$\Sigma_1 \longrightarrow e^{i\tau^a\theta^a}\, \Sigma_1\, e^{-i\tau^3\theta_1' Y_1} \tag{2.36}$$

$$\Sigma_2 \longrightarrow e^{i\tau^a\theta^a}\, \Sigma_2\, e^{-i\tau^3\theta_2' Y_2} \tag{2.37}$$

$$\sigma \longrightarrow e^{i\theta_1' Y_1/2}\, \sigma\, e^{-i\theta_2' Y_2/2}. \tag{2.38}$$

If we now choose the Y_1 and Y_2 charge of the scalar field σ to be p, then the Z' mass will have the same p dependence as in section 2.3. See Table 2.2 for a summary of all charge assignments.

We will now introduce the gauge covariant derivative of the electroweak sector:

$$\partial^\mu + ig\, T^a\, W_a^\mu + ig_1'\, Y_1\, B_1^\mu + ig_2'\, Y_2 B_2^\mu. \tag{2.39}$$

Table 2.2. Gauge Charge Assignments for the different composite fields.

	$SU(N)_{TC}$	$SU(3)_1$	$SU(3)_2$	$SU(2)_W$	$U(1)_1$	$U(1)_2$
Φ_α^β	1	3	$\bar{3}$	1	$p/\sqrt{6}$	$-p/\sqrt{6}$
Σ_1	1	1	1	2	1	0
Σ_2	1	1	1	2	0	1
σ	1	1	1	1	p	p

Since we know that the electric charge operator $Q = T_3 + Y_1 + Y_2$ has to be unbroken and therefore annihilates the vacuum, it will be useful to rewrite (2.39) in terms of the massless EM-field A^μ and the massive Z-boson field. Just like in the Standard Model we introduce the mixing angle θ (its exact correspondence to the observable weak-mixing-angle will be discussed later), $\sin\theta = g'/\sqrt{g^2+g'^2}$, for the mixing of the fields of the second symmetry breaking. Here we again have $g' = g'_1 g'_2/\sqrt{g'^2_1 + g'^2_2}$ for the coupling constant of the hypercharge group $Y = Y_1 + Y_2$ after the first symmetry breaking. For the (first) symmetry breaking at the scale u we already introduced the mixing angle ϕ. We can then write down the mass eigenstate fields

$$Z'_\perp = \cos\phi\, B_2^\mu + \sin\phi\, B_1^\mu$$
$$Z' = -\sin\phi\, B_2^\mu + \cos\phi\, B_1^\mu,$$

after the first symmetry breaking ($Z'_\perp$ denotes the massless gauge boson belonging to the yet unbroken group $Y = Y_1 + Y_2$ and is orthogonal to the massive Z' which we already introduced in section 2.4). Due to the second symmetry breaking we get

$$A^\mu = \cos\theta\, Z'^\mu_\perp + \sin\theta\, W_3^\mu$$
$$Z^\mu = -\sin\theta\, Z'^\mu_\perp + \cos\theta\, W_3^\mu.$$

With the help of the two mixing angles we can also write

$$g = \frac{e}{\sin\theta}, \quad g'_1 = \frac{g'}{\cos\phi} = \frac{e}{\cos\phi\cos\theta}, \quad g'_2 = \frac{g'}{\sin\phi} = \frac{e}{\sin\phi\cos\theta}.$$

Putting everything together and simplifying the result enables us to rewrite the covariant derivative (2.39) as

$$D^\mu = \partial^\mu + ieA^\mu Q + i\frac{e}{\sin\theta\cos\theta}Z^\mu\left(T^3 - \sin^2\theta\, Q\right) + i\frac{e}{\cos\theta\sin\phi\cos\phi}Z'^\mu Y', \quad (2.40)$$

where $Y' \equiv Y_1 - Y\sin^2\phi$ and the $W^\pm$ fields were left out.

Using the transformation properties (2.36 – 2.38) and the charge assignments of Table 2.2 we can now apply this covariant derivative to the vacuum expectation value of our fields:

$$\begin{aligned}
D^\mu\langle\Sigma_1\rangle &= \partial^\mu\langle\Sigma_1\rangle + i\tfrac{e}{\sin\theta\cos\theta}Z^\mu\tau^3\langle\Sigma_1\rangle \\
&\quad - i\tfrac{e}{\cos\theta\sin\phi\cos\phi}Z'^\mu\cos^2\phi\,\tau^3\langle\Sigma_1\rangle \\
D^\mu\langle\Sigma_2\rangle &= \partial^\mu\langle\Sigma_2\rangle + i\tfrac{e}{\sin\theta\cos\theta}Z^\mu\tau^3\langle\Sigma_2\rangle \\
&\quad + i\tfrac{e}{\cos\theta\sin\phi\cos\phi}Z'^\mu\sin^2\phi\,\tau^3\langle\Sigma_2\rangle \\
D^\mu\langle\sigma\rangle &= \partial^\mu\langle\sigma\rangle + i\tfrac{v}{2}\tfrac{e}{\cos\theta\sin\phi\cos\phi}Z'^\mu\langle\sigma\rangle.
\end{aligned}$$

Note that since Q is unbroken, Q annihilates the vacuum. The Lagrangian in the non-linear sigma model we are using reads

$$\mathcal{L} = \frac{F_{TC}^2}{4}\,\mathrm{Tr}\left(D^\mu\Sigma_1\right)^\dagger\left(D_\mu\Sigma_1\right) + \frac{f_t^2}{4}\,\mathrm{Tr}\left(D^\mu\Sigma_2\right)^\dagger\left(D_\mu\Sigma_2\right) + \frac{u^2}{2}\left(D^\mu\sigma\right)^*\left(D_\mu\sigma\right). \quad (2.41)$$

Since we only have one gauged $SU(2)$ group, going to unitary gauge would not set both Sigma fields to one. In terms of Nambu-Goldstone bosons (NGB), this means that only three NGB (which are a linear combination of π_1 and π_2) will become the longitudinal parts of the gauge bosons W^+, W^- and Z to make them massive. In the same manner the NGB coming from the σ-field will make the Z' massive. So one $SU(2)$-triplet will remain in the particle spectrum: the top pions.[8]

We are here only interested in the gauge boson masses and not in the (derivative) coupling terms of the pions, so it is sufficient to only look at the first order term of the Lagrangian by plugging in one for all fields. The W-mass expression is the same as for the

[8]We will not analyze experimental implications of the existence of top pions and just note that they have to be sufficiently heavy to explain why none have been found so far. See [11] for more details.

Standard Model at tree level (apart from the subtlety that we did not relate $\sin\theta$ to observables yet):

$$M_W^2 = \frac{e^2 v^2}{4\sin^2\theta}. \tag{2.42}$$

Omitting the known masses of the photon and W fields, we can now easily calculate the squared mass matrix of the Z and Z' bosons. Setting the fields to one, using $\mathrm{Tr}\,\tau^3\tau^3 = \frac{1}{2}$, $F_{TC}^2 + f_t^2 = v^2$ and $f_t = v\sin\alpha$, we obtain

$$M^2 = \frac{e^2 u'^2}{4\sin^2\theta\cos^2\theta}\begin{pmatrix} x^2 & x^2\frac{\sin\theta}{\sin\phi\cos\phi}\left(\cos^2\alpha - \cos^2\phi\right) \\ x^2\frac{\sin\theta}{\sin\phi\cos\phi}\left(\cos^2\alpha - \cos^2\phi\right) & \frac{\sin^2\theta}{\sin^2\phi\cos^2\phi} \end{pmatrix}, \tag{2.43}$$

where we introduced the small parameter $x^2 = v^2/u'^2 = v^2/(up)^2$, $x^2 \ll 1$, and also used

$$\frac{\sin^2\theta}{\sin^2\phi\cos^2\phi}\left(p^2u^2 + f_t^2\sin^4\phi + F_{TC}^2\cos^4\phi\right) \approx u^2p^2\frac{\sin^2\theta}{\sin^2\phi\cos^2\phi}$$

to get the second diagonal element. Note that the smallness of $x^2 = v^2/u'^2$ will be justified in section 3.3, when we apply experimental bounds from electroweak measurements to our model.

The matrix of (2.43) is of the form

$$\begin{pmatrix} \epsilon & \epsilon' \\ \epsilon' & c \end{pmatrix},$$

with $\epsilon,\ \epsilon' \ll 1$ and c of order 1. A matrix of this form has the eigenvalues (up to second order in ϵ')

$$\lambda_1 = c + \frac{\epsilon'^2}{c} \quad \text{and} \quad \lambda_2 = \epsilon - \frac{\epsilon'^2}{c}, \tag{2.44}$$

and the corresponding eigenvectors

$$v_1 = \begin{pmatrix} \frac{\epsilon'}{c} \\ 1 \end{pmatrix} \quad \text{and} \quad v_2 = \begin{pmatrix} 1 \\ -\frac{\epsilon'}{c} \end{pmatrix}. \tag{2.45}$$

Using (2.45) we can now write down the mass eigenstates of the mass matrix (2.43) in first order of x^2 around $x^2 = 0$:

$$Z^\mu \longrightarrow Z^\mu - x^2\frac{\sin\phi\cos\phi}{\sin\theta}\left(\cos^2\alpha - \cos^2\phi\right)Z'^\mu, \tag{2.46}$$

$$Z'^\mu \longrightarrow Z'^\mu + x^2\frac{\sin\phi\cos\phi}{\sin\theta}\left(\cos^2\alpha - \cos^2\phi\right)Z^\mu. \tag{2.47}$$

To simplify our notation we did not distinguish between the gauge states and the mass eigenstates of Z and Z' so far. From now on we will always mean the above mass eigenstates when we refer to one of the two gauge bosons.

We now use (2.44) to also expand the masses of the Z- and Z'-bosons from the mass matrix to linear order in x^2:

$$M_Z^2 = \frac{e^2 v^2}{4 \sin^2\theta \cos^2\theta} \left(1 - x^2 \left(\cos^2\alpha - \cos^2\phi\right)^2\right). \tag{2.48}$$

To that order, the Z'-mass is just

$$M_{Z'}^2 = \frac{e^2 u'^2}{4 \cos^2\theta \sin^2\phi \cos^2\phi} = \frac{u'^2}{4}\left(g'^2 + g^2\right) \tag{2.49}$$

consistent with eqn. (2.18).

By plugging in the mass eigenstate of the Z boson in our expression for the covariant derivative (2.40), we see that the Standard Model coupling of the Z gets shifted to:

$$g_Z = \frac{e}{\sin\theta\cos\theta}\left[T^3 - Q\sin^2\theta - x^2\left(Y_1 - \sin^2\phi Y\right)\left(\cos^2\alpha - \cos^2\phi\right)\right] \tag{2.50}$$

$$= \frac{e}{\sin\theta\cos\theta}\left[T^3 - Q\sin^2\theta - x^2 Y\,\cos^2\phi\left(\cos^2\alpha - \cos^2\phi\right)\right], \tag{2.51}$$

where in the second line we used that $Y = Y_1$ for all fermions in our Topcolor model. To this level of accuracy the coupling of the Z' does not get shifted, since the tree-level coupling of the Z' will already be suppressed by its large mass:

$$g_{Z'} = \frac{e}{\sin\theta\sin\phi\cos\phi}\left(Y_1 - \sin^2\phi Y\right)$$

$$= \frac{e\cos\phi}{\sin\theta\sin\phi} Y \tag{2.52}$$

Therefore the form of the Z' effective Lagrangian in (2.26) does not change after the second symmetry breaking.

2.6 The Full Gap Equations

We already introduced the Nambu-Jona-Lasinio (NJL) model in section 2.1. But there we did not take into account the $U(1)$ groups. Without these additional groups, we could not

prevent the bottom quark from condensing and at the same time have the desired top quark condensate.

We will here modify the gap equation given in ref. [14] to derive the gap equation which takes into account the Z' interaction. The result is

$$m_f = G_1 \frac{m_f M_{Z'}^2}{8\pi^2}\left[1-\left(\frac{m_f}{M_{Z'}}\right)^2 \ln\left(\frac{M_{Z'}^2}{m_f^2}\right)\right] + G_3 \frac{3m_f M_C^2}{8\pi^2}\left[1-\left(\frac{m_f}{M_C}\right)^2 \ln\left(\frac{M_C^2}{m_f^2}\right)\right], \tag{2.53}$$

where the coefficients G_i are

$$\begin{aligned} G_1 &= \tfrac{8\pi}{M_{Z'}^2}\kappa_1 Y_L^f Y_R^f && \text{for all fermions,} \\ G_3 &= 0 && \text{for leptons,} \\ &= \tfrac{4\pi\alpha_S^2}{M_C^2}\tfrac{1}{\kappa_3} && \text{for quark generations I and II,} \\ &= \tfrac{4\pi}{M_C^2}\kappa_3 && \text{for quark generation III.} \end{aligned}$$

We first observe that in the case $m_f \to 0^+$, eqn. (2.53) reduces to

$$1 = \frac{1}{8\pi^2}\left(G_1 M_{Z'}^2 + 3G_3 M_C^2\right). \tag{2.54}$$

If we want a fermion to condense, the gap equation (2.53) for the corresponding fermion must have a solution for $m_f{>}0$.[9] To figure out for which κ_1 and κ_3 values this is true, we rewrite eqn. (2.53):

$$m_f = \frac{m_f}{8\pi^2}\left(G_1 M_{Z'}^2 + 3G_3 M_C^2\right) - \frac{m_f}{8\pi^2}\left(G_1 M_{Z'}^2 \frac{m_f^2}{M_{Z'}^2}\ln\frac{M_{Z'}^2}{m_f^2} + 3G_3 M_C^2 \frac{m_f^2}{M_C^2}\ln\frac{M_C^2}{m_f^2}\right). \tag{2.55}$$

If $m_f > 0$, the second term of this equation is always negative (or zero), so we can write

$$1 < \frac{1}{8\pi^2}\left(G_1 M_{Z'}^2 + 3G_3 M_C^2\right). \tag{2.56}$$

If, on the other hand, this equation holds, eqn. (2.55) can only have a solution for $m_f > 0$. We therefore only expect a condensation, if eqn. (2.56) holds. Accordingly we expect no condensation, if

$$1 > \frac{1}{8\pi^2}\left(G_1 M_{Z'}^2 + 3G_3 M_C^2\right). \tag{2.57}$$

[9] As in chapter2.1 the case $m_f = 0$ is trivial and always possible, so we will ignore it here.

By plugging in eqn. (2.6), we thus obtain three important (theoretical) constraints for our model: equations (2.58-2.60). Equation (2.58) follows from the fact that we want the top quark to condense; equations (2.59) and (2.60) on the other hand have to be fulfilled in order not to get a bottom quark or τ-lepton[10] condensation, respectively:

$$\kappa_3 + \frac{2}{27}\kappa_1 > \frac{2}{3}\pi, \tag{2.58}$$

$$\kappa_3 - \frac{1}{27}\kappa_1 < \frac{2}{3}\pi, \tag{2.59}$$

$$\kappa_1 < 2\pi. \tag{2.60}$$

The critical κ_1 and κ_3 values belong to the case where we set the left-hand side equal to the right-hand side.

So far we have only taken into account the Z' and Coloron interactions in the NJL Lagrangian which leads to the above gap equations. We will now also consider the electromagnetic and the QCD interaction by using the gauged NJL model. This means to replace the ordinary derivatives in the kinetic term of the NJL model by the covariant derivative and to add a gauge kinetic energy term to the NJL model Lagrangian. We use the result given in ref. [14] for the Simmons and Popovic model and alter it to be applicable to our Topcolor model (i.e. take into account the different gauge charge assignments of the fermions). The result is a slight shift of the equations (2.58-2.60):

$$\kappa_3 + \frac{2}{27}\kappa_1 > \frac{2}{3}\pi - \frac{4}{3}\alpha_S - \frac{4}{9}\alpha_Y, \tag{2.61}$$

$$\kappa_3 - \frac{1}{27}\kappa_1 < \frac{2}{3}\pi - \frac{4}{3}\alpha_S + \frac{2}{9}\alpha_Y, \tag{2.62}$$

$$\kappa_1 < 2\pi - 6\alpha_Y. \tag{2.63}$$

Figure 2.4 shows the resulting gap triangle, where $\alpha_Y(M_Z) = 0.010$ and $\alpha_S(M_Z) = 0.118$ from ref. [16] was used. Within the triangle all above conditions are fulfilled. Going back to eqn. (2.55), we also note that for a non-zero dynamical top mass contribution the

[10] Formally a lepton condensation is not excluded by the NJL model. Nevertheless we will find that this is phenomenologically irrelevant, since experimental constraints (and also the Landau pole constraint) will force us into the region of κ_1 being small.

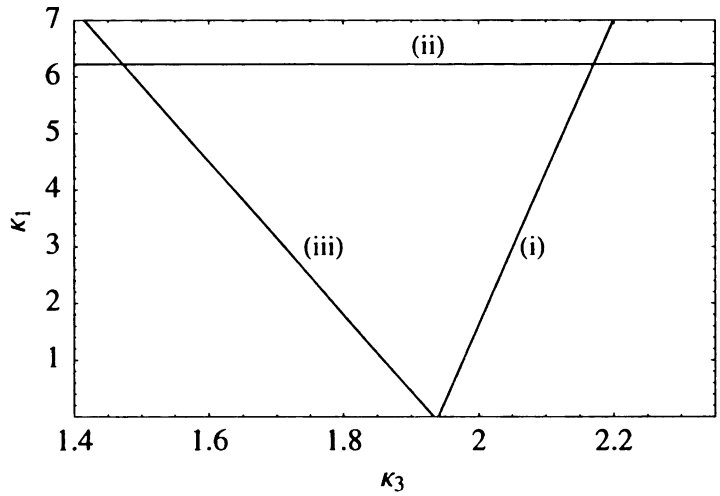

Figure 2.4. Resulting Gap Triangle corresponding to eqns. (2.61-2.63), where (i) is the lower bound for $\langle \bar{b}b \rangle = 0$, (ii) is the upper bound for $\langle \bar{\tau}\tau \rangle = 0$ and (iii) is the lower bound for $\langle \bar{t}t \rangle \neq 0$.

left hand side of the gap triangle is approached in the limit where both gauge boson masses are sent to infinity, corresponding to the case of an infinitely large scale u.

In order not to get a charm condensate, the following condition has to be fulfilled:

$$\kappa_1 + \frac{27}{2}\frac{\alpha_S^2}{\kappa_3} > 9\pi. \tag{2.64}$$

Plugging in $\alpha_S(M_Z) = 0.118$ and using $\kappa_3 \sim 2$ within the gap triangle shows that this does not give a new constraint.

2.7 Implications of the Known Top Mass

We will now briefly discuss that the "smallness" of the top quark mass (compared to the scale u) will result in κ_1 and κ_3 values close to the left hand side of the gap triangle for reasonable scales u. This is analogous to what we found in section 2.1: For a small ratio m_t/u we are forced to couplings close to their critical values.

Using eqns. (2.31) in the gauged version of eqn. (2.53) gives a relation between κ_1 and κ_3 for a given (desired) dynamical fermion mass, a given scale u and a given p. Since the top mass is known to be (174.2 ± 3.3) GeV [16] and the dynamical mass contribution

coming from Extended Technicolor can be estimated to be of the order of the bottom quark mass, i.e. ≈ 5 GeV, we want the Topcolor sector of our model to give a dynamical mass contribution of around 170 GeV.

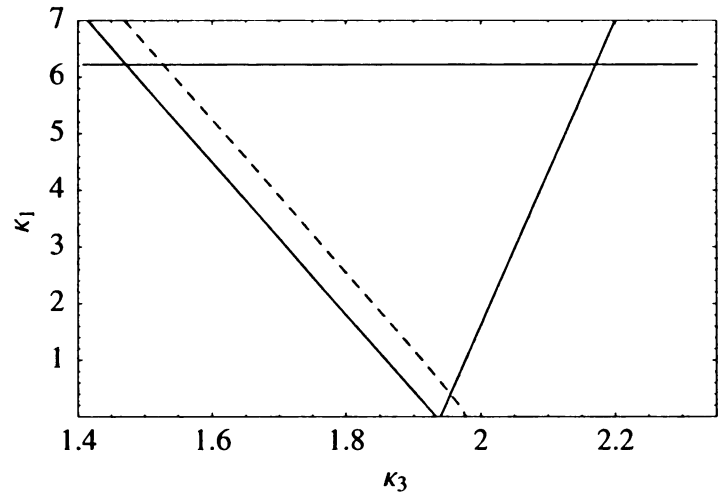

Figure 2.5. The dashed line represents a solution of the gap equation for the scale $u = 500$ GeV using the known top mass of $m_t \approx 170$ GeV. Solutions for higher scales lie to the left of this line.

So using this value for the dynamical top mass, we can now find the solution of the gap equation (2.53) for a given scale u. Note that for simplicity we here assume $p = 1$, so $u = u'$. Fig. 2.5 shows the result for the scale $u = 500$ GeV, which would already be near the electroweak scale v. All solutions for scales above 500 GeV would lie even closer to the left hand side of the gap triangle, which is approached in the limit $u \longrightarrow \infty$.

2.8 The Landau Pole of $U(1)_1$

Just like in QED, one loop corrections because of fermion loops in in the gauge boson propagators will result in a running of the coupling constant g_1' of the $U(1)_1$ group. Since in our Topcolor model, all the fermions only couple to the first $U(1)$ group, there will be no running of the coupling constant g_2'.

It is convenient to choose a renormalization scheme, where the running coupling is

independent of the fermion masses (although in the limit of high energies in which we are interested here, we could neglect the fermion masses anyway), like the $\overline{\text{MS}}$ (modified momentum subtraction) scheme.

Then the beta function, defining the running coupling, is given by

$$\beta(\mu) \equiv \mu \frac{\partial g_1'}{\partial \mu} = C \frac{{g_1'}^3}{12\pi^2}, \tag{2.65}$$

where μ is the energy scale in $\overline{\text{MS}}$ and

$$C = \frac{1}{2} \sum_i Y_i^2 \tag{2.66}$$

is the sum over the squared hypercharges of all fermions (left and right handed) of the Standard Model (since they all transform under $U(1)_1$ with charges equal to their hypercharges in the Standard Model, see table 2.1). The factor $1/2$ is due to the fact that we have to count left- and right-handed fermions separately.

Taking into account all three generations and the color factor of three for the quarks, we find $C = 5$.

Integrating eqn. (2.65) yields the scale dependent coupling at an arbitrary scale Λ, if we know the coupling at another scale Λ_0:

$$g_1'(\Lambda)^2 = g_1'(\Lambda_0)^2 \frac{1}{1 - \frac{C}{6\pi^2} g_1'(\Lambda_0)^2 \ln \frac{\Lambda}{\Lambda_0}}. \tag{2.67}$$

This expression for the running coupling has a pole for $\Lambda = \Lambda_L$, where

$$\Lambda_L = \Lambda_0 \exp\left[\frac{6\pi^2}{C g_1'(\Lambda_0)^2}\right], \tag{2.68}$$

called the Landau pole.

Here we implicitly assumed that the behavior of g_1' outside of perturbation theory can still be described by eqn. (2.65), which is a rather strong assumption. Furthermore we neglect higher order loop correction, which could become important at high scales. Nevertheless, let us assume eqn. (2.65) does describe the high energy behavior of the coupling constant as well. Then the Landau pole scale Λ_L should be at an energy scale well

above the symmetry breaking scale u, since this would then be the energy scale where the theory could not be meaningful anymore. The maximal demand would then be to have Λ_L comparable to the Planck scale, where we expect new physics to become important at the latest.[11]

So let now $\Lambda \approx u$ and let us ask how many orders of magnitude the Landau pole lies above the symmetry breaking scale u, assuming different values of g_1' at u. It is therefore useful to relate g_1' to κ_1 by the use of eqn. (2.27). We then find

$$\log \frac{\Lambda_L}{u} = \log e \, \frac{6\pi^2}{C} \frac{1}{4\pi \left(\kappa_1 + \alpha_Y\right)}, \tag{2.69}$$

where log is the logarithm to basis ten. Requiring Λ_L to lie certain orders of magnitude above u thus gives us an upper bound on κ_1.

The planck scale, $\Lambda_P \approx 1.2\ 10^{16}$ TeV, lies approximately 15 orders of magnitude above the symmetry breaking scale u, if we assume $u \approx 1$ TeV.

Fig. 2.6 shows that if we would want Λ_L to be of the order of Λ_P, this would give us the constraint $\kappa_1 \lesssim 0.02$. In section 3.3.7 we will find that $\kappa_1 \lesssim 0.0015$ has to be fulfilled to assure compliance with electroweak precision data, so the Landau pole does not give us any additional constraint.

2.9 Calculation of the Electroweak Parameters

It is common to express deviations from the SM in terms of the so called electroweak parameters. At first, provided with these parameters we would be able to put constraints on our parameter space without having to calculate every single observable. Secondly, we would then be more flexible to take into account contributions coming from other beyond Standard Models like Extended Technicolor.

To calculate the parameters for our Topcolor model, we will use ref. [4]. It is convenient to use the following parameterization of the tree-level amplitude, which is sufficient to

[11]This is really just a maximum demand. If for example $U(1)_1$ is embedded in the ETC master group, then eqn. (2.67) would actually already loose its meaning above the symmetry breaking scale of ETC.

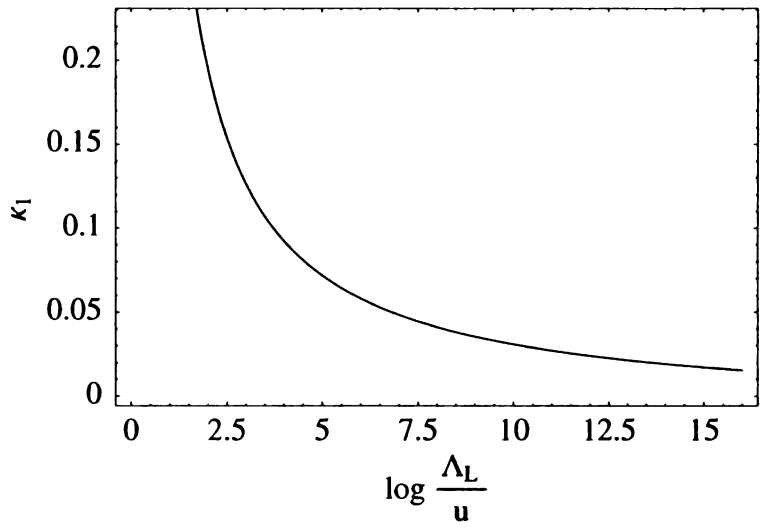

Figure 2.6. The graph shows the upper bound on κ_1, requiring the Landau pole Λ_L to lie certain orders of magnitude above the symmetry breaking scale u.

describe universal corrections to the SM coming from new physics. This parameterization is introduced and explained in ref. [5]. For the neutral current this parametrization reads

$$-\mathcal{M}_{NC} = e^2\frac{QQ'}{P^2} + \frac{(T^3 - s^2Q)(T'^3 - s^2Q')}{\left(\frac{s^2c^2}{e^2} - \frac{S}{16\pi}\right)P^2 + \frac{1}{4\sqrt{2}G_F}\left(1 - \alpha T + \frac{\alpha\delta}{4s^2c^2}\right)} \tag{2.70}$$

$$+ \sqrt{2}G_F\frac{\alpha\delta}{s^2c^2}T^3T'^3 + 4\sqrt{2}G_F(\Delta\rho - \alpha T)(Q - T^3)(Q' - T'^3),$$

whereas the charged current has the following parametrization

$$-\mathcal{M}_{\mathrm{CC}} = \frac{(T^+T'^- + T^-T'^+)/2}{\left(\frac{s^2}{e^2} - \frac{S}{16\pi}\right)P^2 + \frac{1}{4\sqrt{2}G_F}\left(1 + \frac{\alpha\delta}{4s^2c^2}\right)} + \sqrt{2}G_F\frac{\alpha\delta}{s^2c^2}\frac{(T^+T'^- + T^-T'^+)}{2}, \tag{2.71}$$

where we introduced the Euclidean momentum squared $P^2 = -p^2$ to be consistent with [5]. Note that both amplitudes reduce to the SM tree-level currents in the case of vanishing electroweak parameters. In the following we will calculate the electroweak parameters $\Delta\rho$, S, T and δ. We first note that $\delta = 0$ in our model, since we don't have a extra heavy $SU(2)$ triplet.

The neutral current in the model under consideration reads

$$-\mathcal{M}_{NC} = e^2 \frac{QQ'}{P^2} + \frac{g_Z^2}{P^2 + M_Z^2} + \frac{g_{Z'}^2}{M_{Z'}^2}. \tag{2.72}$$

Next, we can rewrite (2.51):

$$\begin{aligned} g_Z =& \frac{e}{\sin\theta\cos\theta}\left[T^3\left(1 + x^2\cos^2\phi\left(\cos^2\alpha - \cos^2\phi\right)\right)\right. \\ & \left. -Q\left(\sin^2\theta + x^2\cos\phi\left(\cos^2\alpha - \cos^2\phi\right)\right)\right] \\ =& \frac{e}{\sin\theta\cos\theta}\left[1 + \Delta_1\right]\left(T^3 - s^2 Q\right), \end{aligned}$$

where we defined

$$\Delta_1 \equiv x^2\cos^2\phi\left(\cos^2\alpha - \cos^2\phi\right) \tag{2.73}$$

for a more readable notation. By comparison to (2.70) we also see that we found s^2 which was implicitly defined there:

$$\begin{aligned} s^2 &= \frac{\sin^2\theta + x^2\cos^2\phi\left(\cos^2\alpha - \cos^2\phi\right)}{1 + x^2\cos^2\phi\left(\cos^2\alpha - \cos^2\phi\right)} \\ &\approx \sin^2\theta + x^2\cos^2\theta\cos^2\phi\left(\cos^2\alpha - \cos^2\phi\right). \end{aligned} \tag{2.74}$$

We now also rewrite (2.48):

$$M_Z^2 = \mu_Z^2\left(1 - \Delta_2\right),$$

where

$$\mu_Z^2 \equiv \frac{e^2 v^2}{4\sin^2\theta\cos^2\theta} \quad \text{and} \quad \Delta_2 \equiv x^2\left(\cos^2\alpha - \cos^2\phi\right).$$

Thus we arrive at the following expression for the Z boson tree-level amplitude:

$$\begin{aligned} \frac{g_Z^2}{P^2 + M_Z^2} &= \frac{e^2}{\sin^2\theta\cos^2\theta}\left(1 + \Delta_1\right)^2 \frac{\left(T^3 - s^2 Q\right)\left(T'^3 - s^2 Q'\right)}{P^2 + \mu_Z^2\left(1 - \Delta_2\right)} \\ &= \frac{\left(T^3 - s^2 Q\right)\left(T'^3 - s^2 Q'\right)}{\frac{\sin^2\theta\cos^2\theta}{e^2(1+\Delta_1)^2}P^2 + \mu_Z^2\frac{\sin^2\theta\cos^2\theta}{e^2}\frac{1-\Delta_2}{(1+\Delta_1)^2}} \end{aligned}$$

In this form we easily get by comparing to (2.70)

$$\frac{s^2 c^2}{e^2} - \frac{S}{16\pi} = \frac{\sin^2\theta\cos^2\theta}{e^2\left(1 + \Delta_1\right)^2}$$

Using s^2 from (2.74) and re-substituting Δ_1 we get to first order in x^2:

$$\alpha S = 4x^2 \left(\cos^2\alpha - \cos^2\phi\right)\cos^2\phi\cos^2\theta \tag{2.75}$$

Next we calculate αT. Again by comparison we find

$$\mu_Z^2 \frac{\sin^2\theta\cos^2\theta}{e^2}\frac{1-\Delta_2}{(1-\Delta_1)^2} = \frac{1}{4\sqrt{2}}(1-\alpha T),$$

where $G_F = \frac{1}{\sqrt{2}v^2}$. Expanding to first order in x^2 yields

$$\alpha T = x^2\left(\cos^4\alpha - \cos^4\phi\right) \tag{2.76}$$

Finally we have to calculate $\Delta\rho$ by looking at the Z' tree-level amplitude:

$$\begin{aligned}\frac{g_{Z'}^2}{M_{Z'}^2} &= x^2\frac{4}{v^2}\cos^4\phi\, YY' \\ &= \frac{4}{v^2}(\Delta\rho - \alpha T)\,YY',\end{aligned}$$

where we used the Z' mass (2.49) and the Z' coupling constant (2.52). Using our result for αT we thus get

$$\Delta\rho = x^2\cos^4\alpha. \tag{2.77}$$

Using again ref. [5] we can translate our result in the Barbieri et al. [2] parametrization of the eletroweak parameters:

$$\widehat{S} = \frac{1}{4s^2}\left(\alpha S + 4c^2(\Delta\rho - \alpha T) + \frac{\alpha\delta}{c^2}\right) = x^2\frac{c^2}{s^2}\cos^2\alpha\cos^2\phi, \tag{2.78}$$

$$\widehat{T} = \Delta\rho = x^2\cos^2\alpha, \tag{2.79}$$

$$W = \frac{\alpha\delta}{4s^2c^2} = 0, \tag{2.80}$$

$$Y = \frac{c^2}{s^2}(\Delta\rho - \alpha T) = x^2\frac{c^2}{s^2}\cos^4\phi. \tag{2.81}$$

Note that there is also a contribution to $\Delta\rho$ coming from loop corrections in the Coloron sector: Coloron exchange across the top and bottom quark loops of the W and Z vacuum polarization diagrams induces the following contribution to $\Delta\rho$ (cf. [14])

$$\Delta\rho^C \approx \frac{16\pi^2\alpha_Y}{3\sin^2\theta_W}\left(\frac{f_t^2}{M_C M_Z}\right)^2\kappa_3. \tag{2.82}$$

But due to the large Coloron mass, this contribution to $\Delta\rho$ turns out to be negligible compared to the tree-level Z' contribution.

2.10 The Weak-Mixing-Angle

Before we can calculate experimental observable deviations from the Standard Model in terms of our four free parameters for the electroweak sector ($[\sin\alpha, \sin\phi, u, p]$ or $[f_t, \kappa_1, u, p]$), we have to relate $\sin\theta$ to observables. To do so, we will reproduce the results given in ref. [4].

There are different possibilities for defining the weak-mixing-angle. In the Standard Model all of them coincide at tree-level, but not at one loop level. For the model we are considering in this thesis, they do not even coincide at tree level.

One possible choice is to define it via the mass ratio of the W and Z masses (the so-called Sirlin definition):

$$\cos^2\theta_W = \frac{M_W^2}{M_Z^2}. \tag{2.83}$$

For our model we find immediately by using eqns. (2.48) and (2.42):

$$\cos^2\theta_W = \cos^2\theta + x^2\cos^2\theta\left(\cos^2\alpha - \cos^2\phi\right)^2, \tag{2.84}$$

or

$$\sin^2\theta_W = \sin^2\theta - x^2\cos^2\theta\left(\cos^2\alpha - \cos^2\phi\right)^2. \tag{2.85}$$

We will later use this result to calculate the W mass shift in our Topcolor model.

Noting that since the best measured electroweak quantities are α, G_F and M_Z, we will find another definition of the weak-mixing-angle more convenient:

$$\sin^2\theta_Z\cos^2\theta_Z = \frac{\pi\alpha}{\sqrt{2}G_F M_Z^2}. \tag{2.86}$$

We will use this definition for the weak-mixing-angle and in general use α, G_F and M_Z as input parameters for all tree-level calculations. For our Topcolor model we have

$$\sin^2\theta_Z\cos^2\theta_Z = \sin^2\theta\cos^2\theta\left(1 + x^2\left(\cos^2\alpha - \cos^2\phi\right)^2\right), \tag{2.87}$$

where we used $v^2 = 1/\sqrt{2}G_F$ and $\alpha = e^2/4\pi$ and the Z mass from (2.48).

This equation can most easily be solved by writing $\sin^2\theta_Z = \sin^2\theta + \Delta\sin^2\theta$, with $\Delta\sin^2\theta$ of order x^2. If we only keep linear terms in $\Delta\sin^2\theta$ we get

$$\Delta\sin^2\theta = x^2\frac{\sin^2\theta\cos^2\theta}{\cos^2\theta - \sin^2\theta}\left(\cos^2\alpha - \cos^2\phi\right)^2$$

and hence

$$\sin^2\theta_Z = \sin^2\theta + x^2\frac{\sin^2\theta\cos^2\theta}{\cos^2\theta - \sin^2\theta}\left(\cos^2\alpha - \cos^2\phi\right)^2. \tag{2.88}$$

It is important to note that the difference between $\sin^2\theta, \sin^2\theta_Z, s^2$ and $\sin^2\theta_W$ are of order x^2, so that any definition of the weak-mixing-angle may be used in the terms proportional to x^2. With this relations we can relate the Lagrangian coupling $\sin\theta$ to measurable quantities.

Chapter 3

Experimental Constraints

3.1 Flavor Changing Neutral Currents: $K\bar{K}$ and $B\bar{B}$ mixing

Our effective Lagrangian, equations (2.25) and (2.26), contains flavor changing neutral currents (FCNC) in first order, since we do not know the complete underlying field theory and therefore can have an arbitrary unitary mixing between the flavors. Equations (2.25) and (2.26) only contain the gauge eigenstates of the theory and thus have to be rotated by a unitary mixing matrix, which could only be derived from the complete theory. Figure (3.1) shows the Feynman diagram for this process. To get an estimate of the size of the FCNC, we will assume a mixing only between the left-handed down quark fields and plug in the CKM-Matrix for this mixing. The fields in the effective Lagrangian are all left-handed, since we assume that only they mix.

$$\mathcal{L} = -\frac{2\pi}{M_C^2}\left[\sqrt{\kappa_3}\left(\bar{b'}_L\gamma^\mu\frac{\lambda^A}{2}b'_L\right) - \frac{\alpha_S}{\sqrt{\kappa_3}}\left(\bar{d'}_L\gamma^\mu\frac{\lambda^a}{2}d'_L + \bar{s'}_L\gamma^\mu\frac{\lambda^a}{2}s'_L\right)\right]^2 \tag{3.1}$$

In equation (3.1), the primed fields denote the gauge eigenstates. We obtain the mass eigenstates by rotating the gauge eigenstates via the CKM-Matrix, $d'^i_L = V^{ij}d^j_L$. Plugging

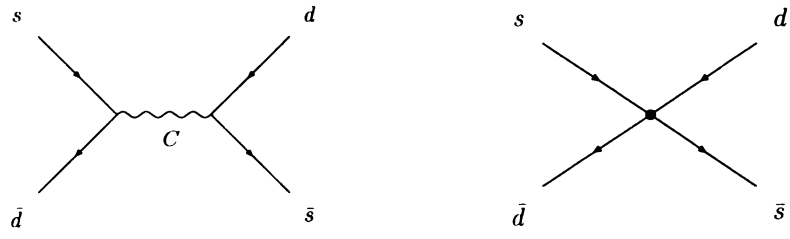

Figure 3.1. (a) shows $K\bar{K}$ mixing in the Top Color model due to Coloron Exchange, (b) shows the corresponding direct coupled diagram.

this transformation into (3.1) yields:

$$\begin{aligned}\mathcal{L} = &-\frac{2\pi}{M_C^2}\left[\sqrt{\kappa_3}\left(\bar{d}_L^j V^{\dagger j3}\gamma^\mu\frac{\lambda^A}{2}V^{3k}d_L^k\right)\right.\\ &\left.-\frac{\alpha_S}{\sqrt{\kappa_3}}\left(\bar{d}^j V^{\dagger j1}{d'}_L\gamma^\mu\frac{\lambda^a}{2}V^{1k}d_L^k+\bar{d}^j V^{\dagger j2}\gamma^\mu\frac{\lambda^a}{2}V^{2k}d_L^k\right)\right]^2\\ = &\ldots-\frac{2\pi}{M_C^2}\left[\sqrt{\kappa_3}V^{\dagger 13}V^{32}-\frac{\alpha_S}{\sqrt{\kappa_3}}\left(V^{\dagger 11}V^{12}+V^{\dagger 12}V^{22}\right)\right]^2\\ &\times\left(\bar{d}_L\gamma^\mu\frac{\lambda^A}{2}s_L\right)^2,\end{aligned} \tag{3.2}$$

where in the last equality we have isolated the terms of interest for $K\bar{K}$-mixing. Here we explicitly see the important difference to flavor universal models like the SM: If the coupling to the three generations was equal, the sum over the factors V^{ij} would equal one due to the unitarity of the mixing matrix. This in generally true: Models which dynamically produce masses (ETC is another example for this) have to couple differently to the three generations and thus will give rise to FCNC.

We thus obtain a coefficient which has a dependence on κ_3 and the CKM-Matrix elements. To simplify equation (3.2) further, the following Fierz identity[1] will be useful:

$$\left(\bar{d}_{L\alpha}\gamma_\mu s_{L\beta}\right)\left(\bar{d}_{L\beta}\gamma^\mu s_{L\alpha}\right) = +\left(\bar{d}_{L\alpha}\gamma_\mu s_{L\alpha}\right)\left(\bar{d}_{L\beta}\gamma^\mu s_{L\beta}\right). \tag{3.3}$$

[1] We have a plus sign on the RHS, because we took into account the extra minus sign from Fermi statistics.

We now use this relation and identity (2.13) for the Gell-Mann matrices to rewrite

$$\begin{aligned}
&\left(\bar{d}_{L\alpha}\gamma_\mu\frac{1}{2}\left(\lambda^A\right)_{\alpha\beta}s_{L\beta}\right)\left(\bar{d}_{L\gamma}\gamma^\mu\frac{1}{2}\left(\lambda^A\right)_{\gamma\delta}s_{L\delta}\right)\\
&=\frac{1}{2}\left(\bar{d}_{L\alpha}\gamma_\mu s_{L\beta}\right)\left(\bar{d}_{L\beta}\gamma^\mu s_{L\alpha}\right)-\frac{1}{6}\left(\bar{d}_{L\alpha}\gamma_\mu s_{L\alpha}\right)\left(\bar{d}_{L\gamma}\gamma^\mu s_{L\gamma}\right)\\
&=\frac{1}{3}\left(\bar{d}_{L\alpha}\gamma_\mu s_{L\alpha}\right)\left(\bar{d}_{L\beta}\gamma^\mu s_{L\beta}\right).
\end{aligned}\tag{3.4}$$

By using this result in the effective Lagrangian, equation (3.2), we obtain the effective Topcolor (Tc) Lagrangian for the $\Delta s = 2$ process under consideration

$$\mathcal{L}^{Tc}_{\Delta s=2} = -\Omega^{Tc}(M_C,\kappa_3)\left(\bar{d}_{L\alpha}\gamma_\mu s_{L\alpha}\right)\left(\bar{d}_{L\beta}\gamma^\mu s_{L\beta}\right),\tag{3.5}$$

where

$$\Omega^{Tc}(M_C,\kappa_3)\equiv\frac{2\pi}{3M_C^2}\left[\sqrt{\kappa_3}V^{\dagger 13}V^{32}-\frac{\alpha_S}{\sqrt{\kappa_3}}\left(V^{\dagger 11}V^{12}+V^{\dagger 12}V^{22}\right)\right]^2.\tag{3.6}$$

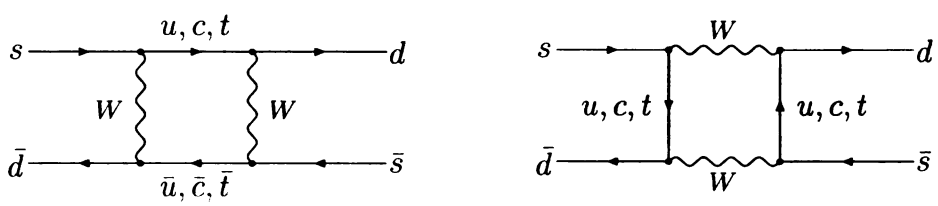

Figure 3.2. Standard Model Loop diagrams for $\Delta s = 2$ transition in $K\bar{K}$ mixing

In the Standard Model (SM) there also exists a $K\bar{K}$ mixing amplitude, but it is strongly suppressed by the GIM-Mechanism and therefore only of second order. The corresponding Feynman diagrams are shown in figure (3.2). A detailed calculation of the involved loop diagrams can be found in [3]. The result is

$$\mathcal{L}^{SM}_{\Delta s=2} = -\Omega^{SM}\left(\bar{d}_{L\alpha}\gamma_\mu s_{L\alpha}\right)\left(\bar{d}_{L\beta}\gamma^\mu s_{L\beta}\right),\tag{3.7}$$

where

$$\Omega^{SM}\equiv\frac{G_F}{\sqrt{2}}\frac{\alpha}{4\pi}\frac{1}{\sin^2\theta_W}\lambda\tag{3.8}$$

and

$$\lambda\equiv\sum_i\left(V^{\dagger 1i}V^{i2}\right)^2 x_i+\sum_{i\neq j}V^{\dagger 1i}V^{i2}V^{\dagger 1j}V^{j2}\frac{x_i x_j}{x_i-x_j}\ln\frac{x_i}{x_j},\tag{3.9}$$

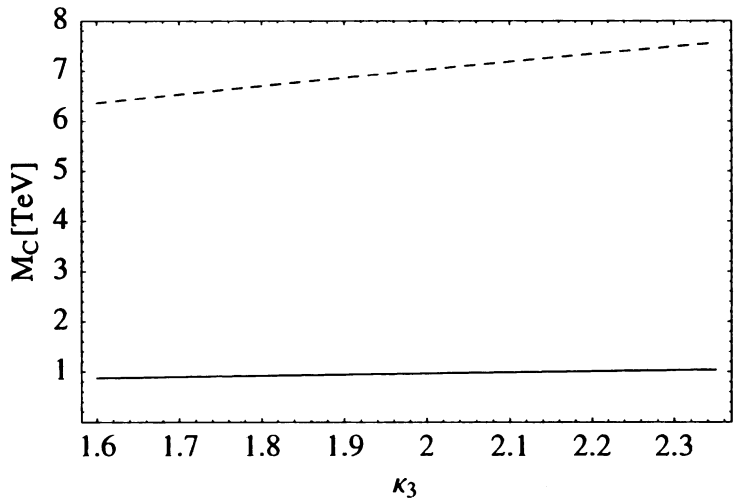

Figure 3.3. Lower bound for M_C due to $K\bar{K}$ (solid line) and $B\bar{B}$ (dashed line) mixing for the allowed values of κ_3

with $x_i \equiv m_i^2/M_W^2$. The indices i, j correspond to up, charm and top quark.

The corresponding relevant observable would now be the mass difference between K^0 and $\bar{K}^0$, which can be estimated from the effective Lagrangian, $\mathcal{L}^{SM}_{\Delta s=2}$ and $\mathcal{L}^{Tc}_{\Delta s=2}$. But since the bound state physics of the involved mesons is not well-understood, this would only be a rather rough estimate. It makes more sense to compare the two factors Ω^{SM} and Ω^{Tc} directly, instead of calculating the sum of both mass difference contributions and comparing this with the observed value.

To do the calculation, we choose the standard parametrization for the CKM matrix. Equation (3.10) shows the measured CKM-Matrix elements, where the phase is omitted and the experimental errors are not taken into account.

$$V \approx \begin{pmatrix} 0.9745 & 0.2243 & 0.0037 \\ -0.2242 & 0.9736 & 0.0413 \\ 0.0057 & -0.0411 & 0.9991 \end{pmatrix} \tag{3.10}$$

The solid line of Fig. 3.3 shows the resulting lower bound on M_C for the NJL model allowed values of κ_3, if we use $\Omega^{SM} \approx \Omega^{Tc}$ and $\alpha_S(M_Z) = 0.118$. Due to this constraint, $M_C \gtrsim 1\,\text{TeV}$.

Exactly the same calculation can be done for $B\bar{B}$ mixing by replacing the quark indices according to $s \longrightarrow d$ and $d \longrightarrow b$. As the dashed line of Fig. 3.3 shows, we get a much stronger constraint for the Coloron mass in this case: $M_C \gtrsim 6 - 8\,\text{TeV}$.

3.2 Limits on Four-Fermion Contact Interactions

LEP 2 measurements of Scale Limits for Four-Fermion Contact Interactions give us a constraint on κ_1. The published analysis of the relevant data assumes an effective Lagrangian of the general form

$$\pm \frac{g^2}{2\Lambda_\pm^2} \left(\bar{\psi}_L \gamma_\mu \psi_L\right) \left(\bar{\psi}_L \gamma^\mu \psi_L\right) = \pm \frac{2\pi}{\Lambda_\pm^2} \left(\bar{\psi}_L \gamma_\mu \psi_L\right) \left(\bar{\psi}_L \gamma^\mu \psi_L\right), \tag{3.11}$$

where $g^2/4\pi$ is assumed to be one. Ref. [16] provides a list of experimental lower bounds

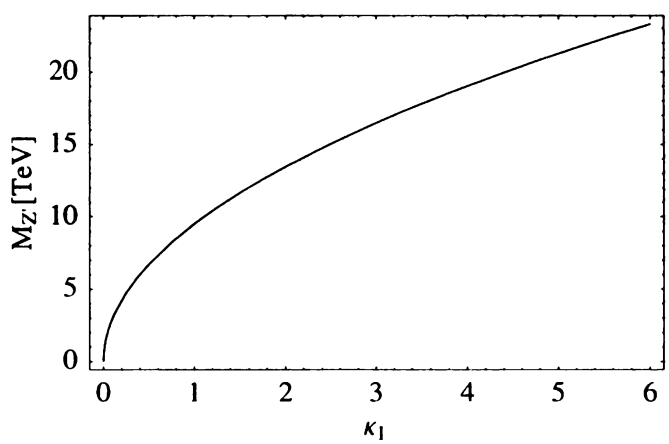

Figure 3.4. Lower bound for $M_{Z'}$ due to scale limits on contact interactions for the allowed values of κ_1.

for $\Lambda_\pm$ for different four fermion interactions. Taking into account the hypercharges, the strongest constraint for our model comes from an (eeuu) interaction. For this interaction we have the following Lagrangian

$$\begin{aligned} \mathcal{L}_{Z'} &= -2\frac{2\pi\kappa_1}{M_{Z'}^2} \left(\bar{e}_L \gamma_\mu Y e_L\right) \left(\bar{u}_L \gamma^\mu Y u_L\right) \\ &= 2\frac{2\pi\kappa_1}{M_{Z'}^2} \frac{1}{12} \left(\bar{e}_L \gamma_\mu e_L\right) \left(\bar{u}_L \gamma^\mu u_L\right), \end{aligned} \tag{3.12}$$

where the factor of two takes into account that we have two equal, (eeuu) and (uuee), effective Lagrangian contributions. Thus we get

$$M_{Z'} \gtrsim \frac{\Lambda_+}{\sqrt{6}}\sqrt{\kappa_1}. \tag{3.13}$$

Figure 3.4 shows the corresponding plot, where the measured $\Lambda_+ > 23.3\,\text{TeV}$ is true for the region above the graph. We see that the Z' mass increases fast with increasing κ_1 values.

3.3 Constraints from Electroweak Precision Measurements

3.3.1 General Considerations

We could now just use the experimental bounds on the electroweak parameters $\widehat{S}, \widehat{T}, Y$ and W obtained from a fit to all relevant available observables to get constraints on our parameter space. Such a fit is provided by Barbieri et al. [2] and we will apply it to our model in section 3.3.7. But we have two good reasons to do our own fit first: to begin with, just translating the constraints on the electroweak parameters does not tell us how well our model is actually fitting the data. This information is hidden in the χ^2_{min} value of a fit in our two parameters κ_1 and u' (if we fix f_t by the Pagel-Stokar formula, see section 2.1). Secondly, it would be interesting to see which observable is causing a strong constraint, and which is not.

We will therefore in this section at first explain the general fitting procedure for the class of models which can be parameterized by the amplitudes (2.70) and (2.71) to understand how Barbieri et al. [2] obtained their general fit in the electroweak parameters. Then we will do our own fit to the Z pole LEP observables to see to what extend our model is able to fit the data. Since we will not include as many observables as Barbieri et al., we will afterwards take the Barbieri fit as the more significant constraint on our parameter space.

Throughout this chapter we will use the following most precisely measured observables as input parameters (at tree level): the QED coupling constant α, the Z mass M_Z and the Fermi constant G_F. See table A.7 for a list of all used input parameters obtained from [16]. By input parameter we here mean that we will not take them as fitting parameters, but fix them to their extremely precise measured mean values. Note that, although all errors are given for a 1-σ confidence level, we will present all bounds on our parameter space at a 95.4% confidence level, corresponding to a 2-σ uncertainty.

Given the great success of the Standard Model, all models beyond the Standard Model have to reproduce it at low energies. In our case this is true for large u. Moreover, deviations

from the Standard Model can only be of order of the Standard Model loop corrections or less, since otherwise they would have been observed already. Since our model would predict deviations from the Standard Model already at tree-level (manifest in the altered Z mass and coupling), these tree-level deviations themselves have to be of the order of the Standard Model one loop corrections. That means we necessarily have to take into account all one loop corrections to the Standard Model when calculating observables in our model. Otherwise we could mistake standard one loop effects for new physics!

We can accomplish this by first calculating the tree-level amplitude, O^{tl}, for the observable O under consideration to first order in x^2 in our model. Since $\sin\theta_Z$ is directly related to the three most precisely measured quantities, we now choose to write everything in terms of $\sin\theta_Z$ by using the relations given in section 2.10. Then the part of the amplitude remaining as $x^2 \longrightarrow 0$ can be identified with the Standard Model tree level amplitude for the given observable, O^{tl}_{SM}:

$$O^{tl} = O^{tl}_{SM} + \delta O_{NP}, \tag{3.14}$$

where δO_{NP} is the small deviation due to new physics, which will be of order x^2. Next we take into account that δO must be comparable to the one loop Standard Model corrections by replacing O^{tl}_{SM} with the best available theoretical prediction of the Standard Model including one loop and radiative corrections, O^{ol}_{SM}:

$$O = O^{ol}_{SM} + \delta O_{NP}. \tag{3.15}$$

In order to get O^{ol}_{SM} we will use the Fortran program ZFITTER [1]. Finally we note, that to this level of accuracy we may equivalently do the following[2]

$$O^{tl} = O^{tl}_{SM}\left(1 + \frac{\delta O_{NP}}{O^{tl}_{SM}}\right) \longrightarrow O = O^{ol}_{SM}\left(1 + \frac{\delta O_{NP}}{O^{tl}_{SM}}\right), \tag{3.16}$$

which sometimes may be more convenient.

[2]We will choose to use this replacement rule. Explicitly doing the calculation also with the replacement (3.15) showed no significant difference in the final fitting results.

Our correction term wouldx now have three independent parameters: $u', \cos\alpha$ and $\cos\phi$. The experimental constraints on the parameter space would be much easier to handle and to illustrate if we had only two independent parameters. Indeed, we can estimate $\cos\alpha$ by the use of the Pagels-Stokar formula (see section 2.1):

$$f_t^2 = \frac{3m_t^2}{8\pi^2} \ln \frac{u^2}{m_t^2} \tag{3.17}$$

and hence

$$\cos^2\alpha = 1 - \frac{3m_t^2}{8\pi^2 v^2} \ln \frac{u^2}{m_t^2}, \tag{3.18}$$

where m_t is the top mass. In our electroweak analysis, we don't have to carry around the dependence on the scale u, since it is only logarithmic and the much more important dependence on the scale is due to $x = \frac{v}{up}$. [3] We will simply fix f_t to $f_t \approx 75$ GeV, which corresponds to $u = 2$ TeV.

Now there is one subtlety: One loop corrections to the Standard Model depend on the unknown Higgs mass, and Technicolor models do not have an elementary Higgs boson. So in our model, too, the Higgs particle needs to be replaced by a particle which plays the role of the Higgs in our theory. To figure out which particle this is, one would have to explicitly do a one loop calculation in our Topcolor model with the triangle moose. For the three-site model this has been done in ref. [13] and the result is that this particle is the techni-ρ meson, which we estimated to weigh around 1.5 TeV in section 1.4. In this thesis we will assume that this is still true in our Topcolor model and use the SM predictions for a heavy Higgs boson mass.

3.3.2 Fits to Electroweak Data

Starting with the charged and neutral current amplitudes (2.70) and (2.71), all electroweak observables may be calculated as functions of S, T, δ and $\Delta\rho$ to first order in these parameters. To do so, one again has to relate s^2, which is implicitly defined in (2.70) and (2.71), to observables. We already did that in the special case of our model in section 2.10.

[3] Not neglecting this scale dependence during the analysis only confirmed this statement.

In order to find the Z boson pole mass from eqn. (2.70), we set the denominator of the Z boson amplitude equal to zero and substitute $Q^2 = -M_Z^2$. To first order in S, we find (cf. [4]):

$$M_Z^2 = \frac{\pi\alpha}{\sqrt{2}G_F s^2 c^2}\left(1 + \frac{\alpha S}{4s^2c^2} - \alpha T + \frac{\alpha\delta}{4s^2c^2}\right). \tag{3.19}$$

And thus

$$\begin{aligned} s^2c^2 &= \frac{\pi\alpha}{\sqrt{2}G_F M_Z^2}\left(1 + \frac{\alpha S}{4s^2c^2} - \alpha T + \frac{\alpha\delta}{4s^2c^2}\right) \\ &= \sin^2\theta_z \cos^2\theta_z \left(1 + \frac{\alpha S}{4s^2c^2} - \alpha T + \frac{\alpha\delta}{4s^2c^2}\right). \end{aligned}$$

Setting $s^2 = \sin^2\theta_z + \delta s^2$ and only keeping terms up to first order in δs^2 we find

$$\delta s^2 = \frac{\sin^2\theta_z \cos^2\theta_z}{\cos^2\theta_z - \sin^2\theta_z}\left(1 + \frac{\alpha S}{4s^2c^2} - \alpha T + \frac{\alpha\delta}{4s^2c^2}\right)$$

and hence

$$s^2 = \sin^2\theta_z + \frac{\sin^2\theta_z \cos^2\theta_z}{\cos^2\theta_z - \sin^2\theta_z}\left(1 + \frac{\alpha S}{4s^2c^2} - \alpha T + \frac{\alpha\delta}{4s^2c^2}\right). \tag{3.20}$$

Using this relation, all observables can be expressed to first order in $S, T, \delta, \Delta\rho$ and the observable $\sin\theta_z$. Thus the theoretical tree-level prediction O_i^{th} for the observable O_i can be put into the following form:

$$O_i^{th} = O_i^{SM} + a_i\alpha S + b_i\alpha T + c_i\alpha\delta + d_i\Delta\rho, \tag{3.21}$$

where O_i^{SM} depends on $\sin\theta_z$ and stands for the tree-level expression in the Standard Model. Now we follow the procedure described in section 3.3.1 and perform the same replacement as in eqn. (3.15): The tree-level prediction from the Standard Model has to be replaced by the one-loop prediction (for example by using the program ZFITTER [1]):

$$O_i^{th} = O_i^{ol} + a_i\alpha S + b_i\alpha T + c_i\alpha\delta + d_i\Delta\rho. \tag{3.22}$$

An appropriate set of observables O_i is given in the appendix, table A.2, for instance. The difficult part is now the calculation of the factors a_i, b_i, c_i and d_i.

Subsequently, one can use the χ^2-method to find the values for $S, T, \Delta\rho$ and δ which fit the data best (actually it is also a matter of definition what a good fit is, but we shall not worry about statistical subtleties too much here) and also the uncertainty of these values for a given confidence level. Although the set of observables in table A.2 is referred to by the LEP working group [6] as being convenient for fitting, since they only have small correlations, one still has to take this correlation into account in the definition of the χ^2 function:

$$\chi^2(S,T,\Delta\rho,\delta) \equiv \sum_{ij} \left(O_i^{th}(S,T,\Delta\rho,\delta) - O_i\right) \left(\sigma^2\right)^{-1}_{ij} \left(O_j^{th}(S,T,\Delta\rho,\delta) - O_j\right), \tag{3.23}$$

where

$$\sigma^2 \equiv \sigma_i \rho_{ij} \sigma_j. \tag{3.24}$$

Here σ_i are the 1-σ errors of the observables O_i and ρ_{ij} is the correlation matrix, which for example for the high energy observables in table A.2 can be found in [6]. In the case of independent (uncorrelated) observables, the correlation matrix is equal to the unity matrix.

Minimizing χ^2 in $S, T, \Delta\rho$ and δ yields the mean values $\langle S\rangle, \langle T\rangle, \langle\Delta\rho\rangle$ and $\langle\delta\rangle$ for which the χ^2-function possesses a minimum:

$$\chi^2_{\min} \equiv \chi^2(\langle S\rangle, \langle T\rangle, \langle\Delta\rho\rangle, \langle\delta\rangle). \tag{3.25}$$

Since the O_i^{th} are linear in $S, T, \Delta\rho$ and δ, the χ^2 function is a quadratic form in these parameters and we can write

$$\Delta\chi^2(S,T,\Delta\rho,\delta) \equiv \chi^2(S,T,\Delta\rho,\delta) - \chi^2_{\min} \tag{3.26}$$

$$= \left(S - \langle S\rangle, T - \langle T\rangle, \Delta\rho - \langle\Delta\rho\rangle, \delta - \langle\delta\rangle\right) \left(\sigma'^2\right)^{-1} \begin{pmatrix} S - \langle S\rangle \\ T - \langle T\rangle \\ \Delta\rho - \langle\Delta\rho\rangle \\ \delta - \langle\delta\rangle \end{pmatrix}. \tag{3.27}$$

The σ'^2-matrix and the mean values together with $\chi^2_{\min}$ thus summarize the results of the whole fitting procedure. Like the σ^2-matrix from above, σ'^2 can be split into a (four by

four) correlation matrix ρ'_{ij} and an error vector σ'_i:

$$\left(\sigma'^2\right)_{ij} \equiv \sigma'_i \rho'_{ij} \sigma'_j. \tag{3.28}$$

Since the diagonal elements of ρ' equal one, the errors σ_i can be easily extracted from σ'.

We now would like to understand how to find regions in the parameter space which correspond to certain confidence levels: Suppose χ^2 depends on M parameters (in our case $M = 4$), and we allow $\nu < M$ of those parameter to vary (meaning we fix $M - \nu$ by some conditions), then every $\Delta\chi^2 < C$, where C is some positive number, defines a ν-dimensional region in our M-dimensional parameter space. Now the theory of χ^2-distributions relates a given desired confidence level, e.g. 68 %, to a value of C which clearly will be ν dependent. A number of C-values for various confidence levels and different free parameters can be found at [16].

If we are just interested in bounds on our specific Topcolor model, we don't have to be that general. We can instead calculate the observables at tree-level in our model analogous to the corresponding Standard Model calculation and just use the different coupling of the Z boson to fermions from eqn. (2.51). Following the procedure discussed in section 3.3.1, we then express the deviation from the Standard Model prediction in terms of our free parameters $u', \cos\alpha$ and $\cos\phi$ to linear order in x^2. We can then fix $\cos\alpha$ using the Pagels-Stokar formula, eqn. (3.18), and perform a χ^2-fit directly in our two left-over free parameters x^2 and $\cos\phi$. This is what we will do explicitly for the set of observables listed in the appendix.

3.3.3 The Mass of the W Boson

The calculation of our first observable, the W mass, is straightforward. We just have to plug (2.88) into (2.84) to get:

$$\cos^2\theta_W = \frac{M_W^2}{M_Z^2} = \cos^2\theta_Z + x^2 \frac{\cos^4\theta_Z \left(\cos^2\alpha - \cos^2\phi\right)^2}{\cos^2\theta_Z - \sin^2\theta_Z}, \tag{3.29}$$

where we also made use of the fact that we are free to replace $\cos\theta$ by $\cos\theta_Z$ in the term proportional to x^2. We can also write this result as

$$M_W^2 = {M_W^{tl}}^2 \left(1 + \left(\frac{v}{u'}\right)^2 \frac{\cos^2\theta_Z \left(\cos^2\alpha - \cos^2\phi\right)^2}{\cos^2\theta_Z - \sin^2\theta_Z}\right),$$

where we recognized $\cos^2\theta_Z M_Z^2$ to be the Standard Model tree-level expression for M_W: ${M_W^{tl}}^2 = \cos^2\theta_Z M_Z^2$. We now have to replace M_W^{tl} by the best Standard Model prediction M^{ol} using ZFITTER:

$$M_W^2 = {M_W^{ol}}^2 \left(1 + \left(\frac{v}{u'}\right)^2 \frac{\cos^2\theta_Z \left(\cos^2\alpha - \cos^2\phi\right)^2}{\cos^2\theta_Z - \sin^2\theta_Z}\right),$$

or, to that order,

$$M_W = M_W^{ol} \left(1 + \frac{1}{2}\left(\frac{v}{u'}\right)^2 \frac{\cos^2\theta_Z \left(\cos^2\alpha - \cos^2\phi\right)^2}{\cos^2\theta_Z - \sin^2\theta_Z}\right). \tag{3.30}$$

Taking into account the experimental error of M_W and fixing $\cos\alpha$ as explained above, we could now calculate an experimental lower and upper bound on $\cos^2\phi$ for every fixed u'. But thereby we would only optimize our parameters to fit this particular observable and neglect all the others. We will therefore choose to calculate more observables and then do a combined χ^2-fit of all observables.

3.3.4 The Z Decay

In this section we would like to calculate the deviations of the Standard Model Z decay width. The Z-fermion interaction term in our theory can be cast into the same form as it appears in the Standard Model:

$$\mathcal{L} = Z_\mu \bar{f}\gamma^\mu \left(g_{Z_L} P_L + g_{Z_R} P_R\right) f, \tag{3.31}$$

where P_L and P_R are the projection operators

$$P_L = \frac{1-\gamma_5}{2} \quad \text{and} \quad P_R = \frac{1+\gamma_5}{2},$$

and g_{Z_L} and g_{Z_R} can be read off from eqn. (2.51). The Standard Model case is reproduced for $x^2 \to 0$, which also means $\cos\theta \to \cos\theta_Z$. Since this is true we can start with the expression for the partial decay width in the Standard Model and simply replace the Standard Model Z boson coupling with (2.51).

Thus the partial Z decay width has the same form as in the Standard Model

$$\Gamma(Z \to \bar{f}f) = \frac{M_Z}{24\pi}\left(g_L^2 + g_R^2\right) \tag{3.32}$$

and the only difference will be due to the x^2 dependence of the Z coupling constant (2.51). Note that we omitted the subscript Z of the coupling constants for notational simplification.

If we now define

$$g^{SM} = \frac{e}{\sin\theta_z \cos\theta_z}\left(T^3 - \sin^2\theta_z\right),$$

we can express the deviation from the Standard Model (which will be of order x^2) as:

$$\delta g_{L/R} = g_{L/R} - g_{L/R}^{SM}.$$

We also define

$$\delta\Gamma = \Gamma - \Gamma^{SM}$$

and thus can write

$$\Gamma = \Gamma^{SM}\left(1 + \frac{\delta\Gamma}{\Gamma^{SM}}\right), \tag{3.33}$$

which already has the desired form of eqn. (3.16). We now only need to calculate $\delta\Gamma/\Gamma^{SM}$, which can easily be done by noting

$$\frac{\delta\Gamma}{\Gamma^{SM}} = \frac{2g_L^{SM}\delta g_L + 2g_R^{SM}\delta g_R}{\left(g_L^{SM}\right)^2 + \left(g_R^{SM}\right)^2}, \tag{3.34}$$

to first order in x^2. Plugging in our expression for the Z coupling and expanding in first order in x^2 we finally find:

$$\Gamma_{ee} = \Gamma^{SM}\left[1 + x^2\left(1.1998\cos^4\alpha - 0.8651\cos^2\alpha\cos^2\phi - 0.3347\cos^4\phi\right)\right], \tag{3.35}$$

for Z decaying to $\bar{e}e$ (or to $\bar{\mu}\mu$, $\bar{\tau}\tau$, since our model is flavor universal).

By summing over all Standard Model particles (leaving out the top quark to which the Z can not decay) we can also calculate the total decay width:

$$\Gamma_Z = \Gamma_{\text{tot}}^{SM}\left[1 + x^2\left(1.5607\cos^4\alpha - 1.503\cos^2\alpha\cos^2\phi + 1.3472\cos^4\phi\right)\right]. \quad (3.36)$$

This expression again has the required form to do the replacement (3.16) by using the ZFITTER result given in table A.1 (this also takes into account the non-negligible phase space factor in the case of the decay to $\bar{\tau}\tau$):

$$\Gamma_Z = \Gamma_{\text{tot}}^{ol}\left[1 + x^2\left(1.5607\cos^4\alpha - 1.503\cos^2\alpha\cos^2\phi + 1.3472\cos^4\phi\right)\right]. \quad (3.37)$$

In addition to the total decay width Γ_Z, experimentalist prefer to express their measurements in terms of the following combinations of decay widths:

- the hadronic pole cross-section

$$\sigma_{\text{had}} \equiv \frac{12\pi}{m_Z^2}\frac{\Gamma_{ee}\Gamma_{\text{had}}}{\Gamma_Z^2},$$

  where

$$\Gamma_{\text{had}} \equiv \sum_{q\neq t}\Gamma_{q\bar{q}}; \quad (3.38)$$

- the ratios

$$R_e \equiv \Gamma_{\text{had}}/\Gamma_{ee}, \quad R_\mu \equiv \Gamma_{\text{had}}/\Gamma_{\mu\mu} \quad \text{and} \quad R_\tau \equiv \Gamma_{\text{had}}/\Gamma_{\tau\tau},$$

  which reduce to

$$R_\ell \equiv \Gamma_{\text{had}}/\Gamma_{\ell\ell},$$

  if lepton universality is assumed;

- and in the case of a decay to quark-antiquark pairs

$$R_q \equiv \Gamma_{q\bar{q}}/\Gamma_{\text{had}}, \quad \text{e.g. } R_b = \Gamma_{b\bar{b}}/\Gamma_{\text{had}}.$$

3.3.5 Left/Right and Forward/Backward Asymmetries

Another set of strong constraints are due to measurements of the left/right and forward/backward asymmetries.

Using the notation of ref. [6], we quickly review what is meant by and how it comes to asymmetries. As we already saw in eqn. (3.31), the Z couples different to left- and right-handed fermions. If we now consider a positron-electron collider like the SLC (Stanford Linear Collider), cross sections for the process $e\bar{e} \to f\bar{f}$ will depend largely on Z exchange diagrams and therefore be dependent on the polarization of the initial electron and positron beam. Due to the different coupling of the left and right-handed electrons and positrons to the Z boson, the following measurable left/right and forward/backward asymmetries will be non-zero:

$$A_{\mathrm{LR}} \equiv \frac{\sigma_{\mathrm{L}} - \sigma_{\mathrm{R}}}{\sigma_{\mathrm{L}} + \sigma_{\mathrm{R}}} \frac{1}{\langle |\mathcal{P}_e| \rangle} \tag{3.39}$$

$$A_{\mathrm{FB}} \equiv \frac{\sigma_{\mathrm{F}} - \sigma_{\mathrm{B}}}{\sigma_{\mathrm{F}} + \sigma_{\mathrm{B}}}, \tag{3.40}$$

where the capital letters L and R refer to the polarization of the initial electron beam (the positron beam is assumed to be unpolarized) and the cross-sections for forward and backward scattering relatively to the beam axis are denoted σ_{F} and σ_{B}, respectively. Finally, $\mathcal{P}_e$ is the electron beam polarization (between minus one and zero for left-handed polarization and between zero and one in the right-handed case).

In the case of Z decaying to $\tau\bar{\tau}$, we can additionally define the polarization of a $\tau\bar{\tau}$ final state:

$$\mathcal{P}_\tau \equiv \frac{\sigma_{\mathrm{r}} - \sigma_{\mathrm{l}}}{\sigma_{\mathrm{r}} + \sigma_{\mathrm{l}}}, \tag{3.41}$$

where the lower-case letters l and r refer to the polarization of the *final* state τ-lepton.

Without proof we just note (see ref. [6] for a derivation) the following relations which

are valid in the Standard Model:

$$A_{\mathrm{FB}}^{f} = \frac{3}{4}\mathcal{A}_e\mathcal{A}_f \tag{3.42}$$

$$A_{\mathrm{LR}}^{f} = \mathcal{A}_f \tag{3.43}$$

$$\mathcal{P}_\tau = -\mathcal{A}_\tau, \tag{3.44}$$

where

$$A_f \equiv \frac{g_{\mathrm{Lf}}^2 - g_{\mathrm{Rf}}^2}{g_{\mathrm{Lf}}^2 + g_{\mathrm{Rf}}^2}. \tag{3.45}$$

Whereas the left/right Asymmetries A_{LR} were directly measured by SLD (Stanford Large Detector), the polarization $\mathcal{P}_\tau$ and the forward/backward asymmetries were directly measured by LEP (Large Electron Positron Collider). LEP indirectly measured the left/right asymmetries by assuming the validity of eqn. (3.42) and using the SLD measurement of A_{LR}^{e}.

Using again the shifted Z boson coupling (2.51) and the relations (3.42-3.44) we can, an analogy to the calculation of the partial Z decay widths, easily derive the correction factors $\left(1 + O(x^2)\right)$ for all measured asymmetries.

3.3.6 Combined Fit to the Calculated Observables

Now that we have calculated all the different observables in the last sections, we would like to see how the experimental measurements of those observables constrain our parameter space. We will therefore in this section use the experimental values for the flavor universal case given in the appendix and the ZFITTER results for the Standard Model one-loop predictions given in table A.1 to perform a combined fit of all observables listed in the appendix (flavor universal case) to the experimental data.

As mentioned earlier, all ZFITTER (Standard Model) predictions will depend on the Higgs mass, which we would have to replace by the techni-ρ mass at the TeV-scale in our model (see section 3.3). But since the Higgs mass dependence will be approximately logarithmic, we will not make a large mistake, if we take the Higgs mass input of ZFITTER

to be 800 GeV. We choose the particular value of 800 GeV, because Barbieri et al. provide a fit of the electroweak parameters for this Higgs mass and we would like to produce comparable results. We will also see to what extent our result changes when we use the much larger Higgs of 1500 GeV which is closer to the techni-ρ mass we estimated via up-scaling of QCD in section 1.4.

It is now convenient to define χ^2 as a function of $\cos^2\phi$ and x^2 ($\cos\alpha$ is not treated as a free parameter, but fixed by eqn. (3.18)). Taking into account all correlations given in the appendix, the χ^2 function is now defined exactly the way we showed it for the general case in eqn. (3.23). Note that the fit is linear in x^2, but due to the occurrence of $\cos^4\phi$, non-linear in $\cos^2\phi$.

The search for the global minimum of the χ^2 function in the *physically allowed region* of the two parameters ($x^2 \geq 0$ and $0 \leq \cos^2\phi \leq 1$) reveals that the minimum is actually on the boundary at $\cos^2\phi = 0$ and $x^2 = 0.0037$ corresponding to a $\chi^2_{\text{min}} = 15.76$. For $\cos^2\phi$ very near to the boundary $\cos^2\phi = 0$, we can neglect the $\cos^4\phi$ term in the χ^2 function which of course also does not change the χ^2_{min} value. Our fit can therefore be treated as an approximately linear fit, although we will not explicitly set $\cos^4\phi = 0$, which would slightly alter the final upper bound on $\cos^2\phi$ (it would turn out to be a little smaller) if we look at $\Delta\chi^2$. This is important for the statistical interpretation of χ^2_{min} and $\Delta\chi^2$, since one has to assume linearity in the fitting parameters to do so in a statistically well-defined way.

Fig. 3.5 summarizes the whole fitting procedure: For each observable the best fit result and the pull, defined as the difference between the best fit value and the measurement in units of the experimental uncertainty, is shown. Large pulls signal a large contribution to χ^2_{min}.

The pulls are comparable to the SM fitting result which can be found in ref. [6]. Since we have 13 observables and do a fit in two parameters, the degree of freedom (d.o.f.) is $(13-2)$ and $\chi^2_{\text{min}}/\text{d.o.f.} = 1.43$. This value should be near one, and the theory of χ^2 distributions relates this value to a probability in the following sense: Imagine a world

Experimental Value	Fit	Pull
Γ_Z= (2.4952±0.0023) GeV	2.4982 GeV	
σ_{had}= (41.540±0.037) nb	41.485 nb	
R_l= 20.767±0.025	20.747	
A^l_{FB}= 0.0171±0.0010	0.0159	
M_W= (80.403±0.029) GeV	80.406 GeV	
P_τ= 0.1465±0.0033	0.1460	
A^l_{LR}(SLD)= 0.1513±0.0021	0.1460	
R_b= 0.21629±0.00066	0.21580	
R_c= 0.1721±0.0030	0.1722	
A^b_{FB}= 0.0992±0.0016	0.1023	
A^c_{FB}= 0.0707±0.0035	0.0731	
A^b_{LR}= 0.923±0.020	0.9346	
A^c_{LR}= 0.670±0.027	0.6677	

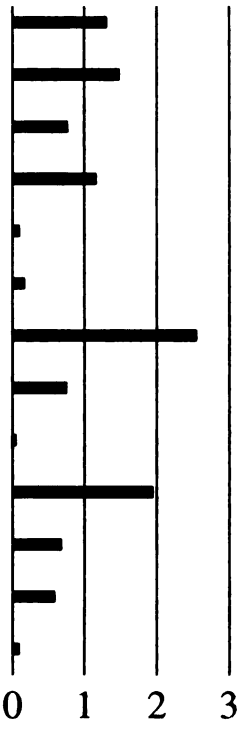

Figure 3.5. Comparison of the experimental values and the best fit prediction of our Topcolor model corresponding to $\chi^2_{\text{min}}/\text{d.o.f.} = 15.76/(13-2) = 1.43$ using a Higgs mass of 800 GeV. Also shown is the pull of each measurement, which is defined as the difference between measurement and expectation over the uncertainty of the measurement.

in which the model you consider is right, meaning experiments in this world could be accurately described with this model. Then the above mentioned probability tells you how likely it is to have a measurement with given uncertainty which gives a $\chi^2_{\text{min}}/\text{d.o.f.}$ bigger than the one you found. For $\chi^2_{\text{min}}/\text{d.o.f.} = 1.43$ this probability is 15.1%.

We would now like to compare this to the Standard Model fit. There is no obvious way to do so. We will choose to fix all predictions of the SM (for the same 11 observables we used in the other fit) to values calculated with ZFITTER with the input parameters given in table A.7. We can then do a one parameter fit for the Standard Model treating the Higgs mass as a free parameter which is just constrained to be greater than 115 GeV due to direct searches. Of course the χ^2_{min} is then found for $m_h = 115$ GeV and we obtain

$\chi^2_{\text{min}}/\text{d.o.f.(SM)} = 16.56/(13-1) = 1.38$. This value corresponds to a probability of 20.2%, which is slightly better, but comparable to the result of the above fit for our Topcolor model.

It is remarkable that our electroweak fitting result is comparable to the SM, because the plain SM fit with a Higgs mass of 800 GeV for the same 13 observables would give a very bad fit with a χ^2_{min} around 100. Repeating the fit for our Topcolor model for a Higgs mass of 1500 GeV also gives a good fit: $\chi^2_{\text{min}}/\text{d.o.f.} = 16.09/(13-2) = 1.46$.

We now define $\Delta\chi^2 = \chi^2 - \chi^2_{\text{min}}$ and use eqn. (2.34), to replace the free parameter $\cos\phi$, which was convenient for the intervening calculations, again by the parameter κ_1:

$$\cos^2\phi = \frac{\kappa_1}{\kappa_1 + \alpha_Y}. \tag{3.46}$$

Working at a confidence level of 95.4% and with two free parameters, we find for example in ref. [16], our restriction on the parameter space to be (compare to section 3.3.2)

$$\Delta\chi^2(\kappa_1, u') < 6.17. \tag{3.47}$$

Fig. 3.6 shows the result for two different Higgs masses: For each Higgs mass the region outside the parabola shaped line is excluded at a confidence level of 95.4% (taking into account all observables under the assumption of lepton flavor universality listed in the appendix).

The lower bound we obtain on u' is found to be approximately 3.5 TeV, with little dependence on the chosen Higgs mass. This justifies our assumption that $x^2 = v^2/u'^2 \ll 1$ in section 2.5. In fact, we find $x^2 \lesssim 0.005$ according to this constraint. We now also obtain an upper bound on the scale of approximately 4.5 TeV, which seems to depend a little more on the chosen Higgs mass. We finally observe that the allowed κ_1 region is bounded from above: $\kappa_1 \lesssim 1 \times 10^{-3}$.

At first sight it seems strange that we obtain an upper bound on the scale. Since the Standard Model would be reproduced for $u' \to \infty$, this means that the Standard Model must not fit the data well. The reason for this can be seen in the (for the Standard Model)

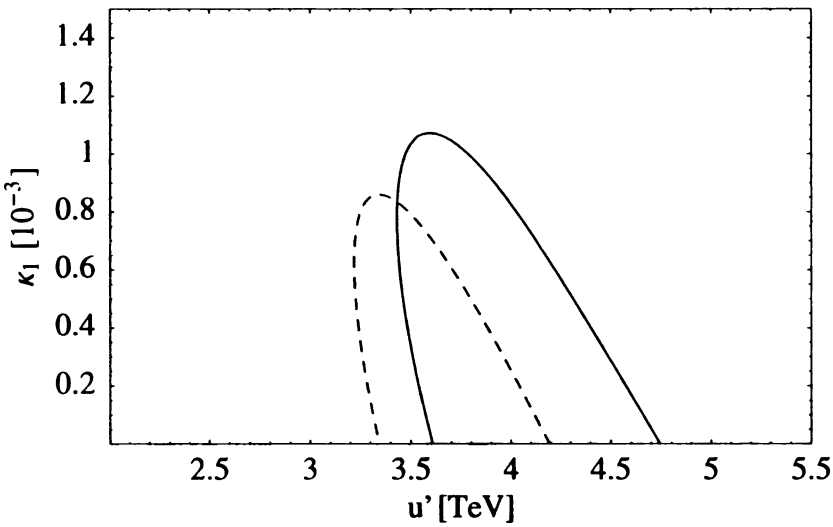

Figure 3.6. Restriction on our parameter space obtained from a fit of all Z pole observables listed in the appendix for two different Higgs masses: $m_h = 800$ GeV (solid line) and $m_h = 1500$ GeV (dashed line). For each Higgs mass the region outside the parabola shaped region is excluded at a confidence level of 95.4%.

unnaturally high Higgs mass. As is well known [6], the Standard Model fits the current data best for a (already excluded) Higgs mass of approximately 80 GeV. If we used a lighter Higgs mass of order 80 GeV, the upper bound on our scale would of course vanish.

To get the desired top condensate and at the same time avoiding bottom quark and tau lepton condensates has led us in section 2.6 to the gap triangle in the κ_3-κ_1 plane (Fig. 2.4). Moreover, as we discussed in section 2.7, the known top mass forces κ_1 and κ_3 to lie in regions very near the left hand side of the gap triangle at scales of the order 1 TeV. We have now found that $u' \gtrsim 3$ TeV and also that $\kappa_1 \lesssim 6 \times 10^{-3}$. This means that in the NJL model approximation we are now restricted to the far tip of the gap triangle at regions very near the left hand side of the gap triangle.

Plugging in eqns. (2.31) for the Z' and Coloron masses and the desired dynamical top mass contribution from Topcolor, $m_t \approx 170$ GeV, into the gauged version of eqn. (2.53) would now enable us to calculate κ_3 for a given value of κ_1, u' and p.[4] In some sense we

[4]The p dependence is due to the fact that the Coloron mass appearing in the gap equation (2.53) is dependent on p for fixed u'.

could thereby translate our constraint from above into the corresponding constraint in the κ_3-κ_1 plane.

Keeping in mind that this translation depends strongly on the reliability of the NJL model, we no longer speak of excluded regions at a certain confidence level. Instead we will look again at the solutions to the gap equation (2.53) belonging to the bounds on the scale we just found: The solid lines in Fig. 3.7 represent the tip of the gap triangle. The

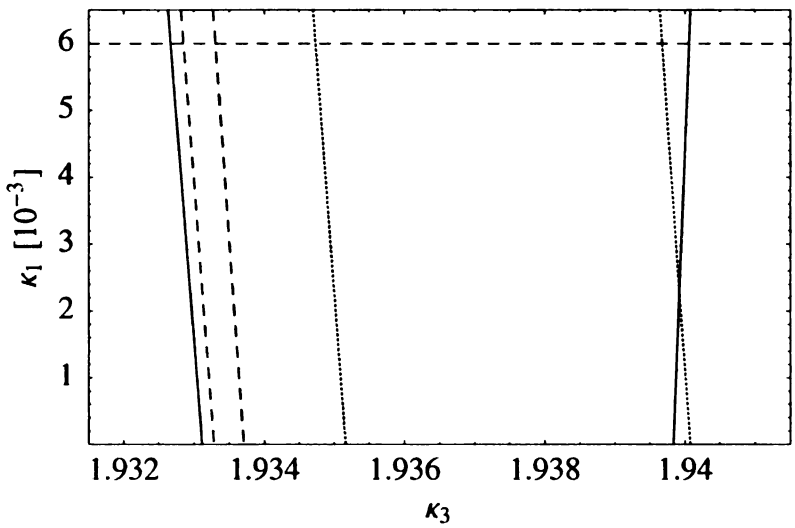

Figure 3.7. The dashed horizontal line illustrates the upper bound on κ_1 and the other lines are solutions to the gap equation belonging to the scales $u = 3$ TeV (right) and $u = 6$ TeV (left) for $p = 0.5$ (dashed lines) and $p = 2$ (dotted lines).

dashed horizontal line illustrates the upper bound on κ_1 and the other lines are solutions to the gap equation belonging to the scales $u = 3$ TeV and $u = 6$ TeV for $p = 0.5$ (dashed lines) and $p = 2$ (dotted lines). Increasing the scale means approaching the left hand side of the triangle. So the naive use of the NJL model gap equation would restrict κ_3 to lie in the narrow band between the dashed lines if we choose $p = 0.5$ and in between the dotted lines if we choose $p = 2$. Solutions for the same scales for smaller p would lie even closer to the left hand side of the triangle and the opposite is true for greater p. The corresponding lines for $p > 3$ would even lie outside the right hand side of the triangle.

Although we should not at all rely on the exact values of κ_3 obtained this way, we can

still conclude that for such small κ_1 values, the possible region for κ_3 allowing a top quark but not a bottom quark condensate is very narrow.

INTERPRETATION IN TERMS OF PESKIN'S ELECTROWEAK PARAMETERS

The resulting bounds on the parameter space we obtained in this section are easy to understand in terms of the Peskin parametrization of the electroweak parameters which we calculated in section 2.9:

$$\alpha S = 4x^2 \left(\cos^2\alpha - \cos^2\phi\right) \cos^2\phi \cos^2\theta$$
$$\alpha T = x^2 \left(\cos^4\alpha - \cos^4\phi\right)$$
$$\Delta\rho = x^2 \cos^4\alpha.$$

Due to the fact that the best fit value for $\cos^2\phi$ is zero, $\Delta\rho \approx \alpha T$ and $S \approx 0$. Fixing $\cos^2\alpha$ by the Pagel-Stokar relation, eqn. (3.18), gives $T \approx 0.4$ for the best fit value $x^2 = 0.0037$.

The experimental bounds on S and T are commonly illustrated as an ellipse in the S-T plane for a reference Higgs mass[5]. Some of these plots[6] also show how the Standard Model contributions to these parameters become non-zero and leave the experimental bounds for very large Higgs masses. For a Higgs mass of around 1 TeV the necessary value of T (coming from physics beyond the Standard Model) to get back into the experimental allowed region is $\sim +0.4$. See ref. [6].

3.3.7 Constraints From the Barbieri et al. Fit

We now would like to see how much the constraint on our parameter space gets altered if we take into account the full set of available precision measurements which is included in the fit of Barbieri et al. [2]. Barbieri et al. [2] use $\widehat{S}, \widehat{T}, W$ and Y as electroweak parameters. Their relation to the parameters $S, T, \Delta\rho$ and δ we used so far, was already given in eqns. (2.78-2.81).

[5]Leaving aside $\Delta\rho$ for the moment.

[6]See for example Fig. E.2 in ref. [6].

The observables used by the electroweak fit of Barbieri et al. [2] are summarized in table A.2. Additionally they included the data of LEP2 for the cross-sections for $e\bar{e} \to e\bar{e}, \mu\bar{\mu}, \tau\bar{\tau}, \sum_q q\bar{q}$ cross sections at $\sqrt{q^2} \approx 189, 192, 196, 200, 202, 205, 207\,\text{GeV}$.

Continuing to use our notation from section 3.3.2, the result of the fit of Barbieri et al. can be summarized by the correlation matrix (the order will always be $\widehat{S}, \widehat{T}, Y$ and W)

$$\rho' = \begin{pmatrix} 1 & 0.68 & 0.65 & -0.12 \\ 0.68 & 1 & 0.11 & 0.19 \\ 0.65 & 0.11 & 1 & -0.59 \\ -0.12 & 0.19 & -0.59 & 1 \end{pmatrix}, \tag{3.48}$$

by the mean values $\langle\widehat{S}\rangle, \langle\widehat{T}\rangle, \langle Y\rangle$ and $\langle W\rangle$ and by the errors σ'_i given in table 3.1.

Higgs mass	$10^3\langle\widehat{S}\rangle$	$10^3\langle\widehat{T}\rangle$	$10^3\langle Y\rangle$	$10^3\langle W\rangle$
$m_h = 115\,\text{GeV}$	0.0 ± 1.3	0.1 ± 0.9	0.1 ± 1.2	-0.4 ± 0.8
$m_h = 800\,\text{GeV}$	-0.9 ± 1.3	2.0 ± 1.0	0.0 ± 1.2	-0.2 ± 0.8

Table 3.1. The mean values and 1-σ errors from the Barbieri et al. fit [2].

By using eqn. (3.27) we thus obtain $\Delta\chi^2$ as a function of $\widehat{S}, \widehat{T}, Y$ and W:

$$\Delta\chi^2\left(\widehat{S}, \widehat{T}, Y, W\right) = \left(\widehat{S} - \langle\widehat{S}\rangle, \widehat{T} - \langle\widehat{T}\rangle, Y - \langle Y\rangle, W - \langle W\rangle\right)\left(\sigma'^2\right)^{-1}\begin{pmatrix} \widehat{S} - \langle\widehat{S}\rangle \\ \widehat{T} - \langle\widehat{T}\rangle \\ Y - \langle Y\rangle \\ W - \langle W\rangle \end{pmatrix}, \tag{3.49}$$

where σ'^2 was defined in (3.28).

Using the fact that in terms of order x^2 we don't have to distinguish between the different definitions of the weak-mixing-angles, we can rewrite eqns. (2.78-2.81):

$$\widehat{S} = \frac{v^2}{u'^2}\frac{\cos^2\theta_z}{\sin^2\theta_z}\frac{\kappa_1}{\kappa_1 + \alpha_Y}\cos^2\alpha \tag{3.50}$$

$$\widehat{T} = \frac{v^2}{u'^2}\cos^2\alpha, \tag{3.51}$$

$$W = 0, \tag{3.52}$$

$$Y = \frac{v^2}{u'^2}\frac{\cos^2\theta_z}{\sin^2\theta_z}\left(\frac{\kappa_1}{\kappa_1 + \alpha_Y}\right)^2, \tag{3.53}$$

where we also used $\cos^2\phi = \frac{\kappa_1}{\kappa_1+\alpha_Y}$ from eqn. (2.34), and $x = v/u'$.

If we now again fix $\cos^2\alpha$ by the Pagels-Stokar formula as described in section 3.3.1, we can plug these equations into (3.49) to obtain $\Delta\chi^2$ as a function of the *two* free parameters κ_1 and u'.

Having two free parameters and working with a confidence level of 95%, we again have[7] (as in eqn. (3.47))

$$\Delta\chi^2\Big(\widehat{S}(\kappa_1,u')\,,\widehat{T}(\kappa_1,u')\,,Y(\kappa_1,u')\,,W=0\Big) < 6.17, \tag{3.54}$$

as a restriction on our parameter space.

Since the Higgs-replacing particle, the techni-ρ, can be estimated to have a mass at the TeV-scale (see section 1.4), we will use the mean values and errors given for the Higgs mass of 800 GeV in table 3.1. Fig. 3.8 shows the result: The region outside the solid, parabola shaped line is excluded at a confidence level of 95%.

Fig. 3.8 also shows the constraint we calculated in the last section, but this time using exactly Barbieri's data given in table A.2. Note that the LEP data Barbieri used was preliminary at that time and that moreover the mean value for the top mass changed significantly. Also the W mass measurement improved due to more recent Tevatron measurements. Comparing the dashed line in Fig. 3.8 with the solid one in Fig. 3.6, it is nevertheless remarkable that the slight change in the used data gives a notable change on the constraint on our parameter space (it becomes slightly weaker).

Also remarkable is the fact that the additional LEP2 cross-sections and the low energy precision data which are also included in the Barbieri et al. fit, slightly relaxes the constraint we already found. This happens if the pulls of the additional included data are smaller than the average pulls of the already included data. Another difference between our analysis from the last section and the Barbieri fit is the different treatment of the radiative corrections to the SM: Barbieri et al. did not use ZFITTER. Taking these differences into account, the

[7]Note that $\Delta\chi^2(\widehat{S},\widehat{T},Y,W)$ has again to be minimized when expressed in κ_1 and u' and the minimum has to be subtracted.

two fits are remarkably consistent.

The whole analysis shows that the parameter space constraints are dependent on the data we choose to include and also a little on the value we choose for the Higgs mass. Nevertheless all fits (with little dependence on the Higgs mass) consistently show $u' \gtrsim 3.5$ TeV. The upper bound on the other hand has a stronger dependence on the Higgs mass and we conclude $u' \lesssim 5 - 6.5$ TeV.

We should note that in this analysis we did not include the (small) contributions to the electroweak parameters coming from Extended Technicolor. So the allowed parameter region obtained here should be viewed as the largest possible.

For the implications of this constraint on allowed regions in the gap triangle in the κ_3-κ_1 plane, there are no new insights compared to what we already concluded in section 3.3.6.

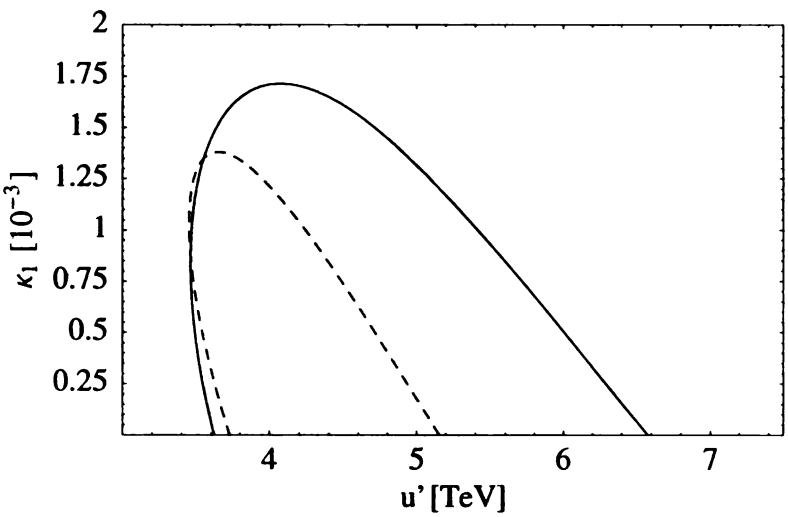

Figure 3.8. 95% confidence level constraint from the full electroweak fit of Barbieri et al. [2] for $m_h = 800$ GeV (solid line). For comparison, the dashed line shows the constraint from last section, but this time using exactly the data of Barbieri et al.

THE Z' MASS

It is now instructive to translate the constraint on the scale u' into a constraint on the Z' mass, using eqn. (2.31):

$$u' = M_{Z'}\sqrt{\frac{\kappa_1}{\pi}}\frac{1}{\kappa_1 + \alpha_Y}. \tag{3.55}$$

The result is shown in Fig. 3.9. We observe that Z' masses less than 2 GeV are excluded at

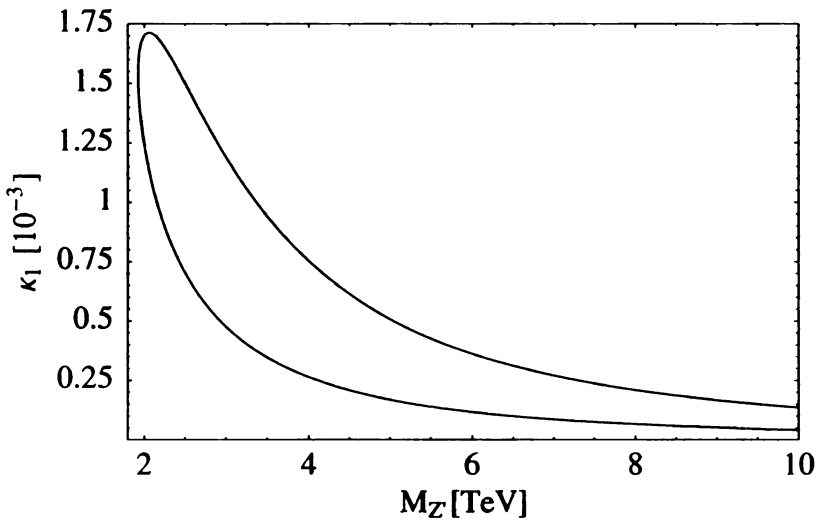

Figure 3.9. Constraint from the electroweak fit of Barbieri et al. for $m_h = 800$ GeV translated into a constraint on the Z' mass.

a confidence level of 95% when using a Higgs mass of 800 GeV. Due to our results from section 3.3.6 we may expect that for a greater Higgs mass (which may be more appropriate, since the techni-ρ meson has a mass at the TeV-scale) this bound relaxes a little. We do not observe an upper bound for $M_{Z'}$ since $M_{Z'} \propto 1/\sqrt{\kappa_1}$ for κ_1-values small compared to $\alpha_Y \approx 0.01$, as can be inferred from eqn. (2.31). Since the best fit value of κ_1 is zero, experiment clearly favors a heavy Z'.

THE COLORON MASS

Finally let us also look at the Coloron mass. The result from the NJL model gap equations was that κ_3 has to be approximately two and for κ_1 being small we have $\kappa_3 \approx 1.9$. Ex-

amining eqn. (2.31) for the Coloron mass as a function of κ_3 and the scale u, we find that in this region of $\kappa_3 \approx 2$, the mass is not much dependent on κ_3. Fixing κ_3 to $\kappa_3 \approx 2$ and allowing u' to vary between four and six TeV, we can estimate the Coloron mass to lie between 20 and 30 TeV, if we choose $p = 1$.

Chapter 4

The Simmons and Popovic Topcolor Model

In this chapter we would like to briefly look at the Simmons and Popovic Topcolor assisted Technicolor model. This model is exactly identically to our model, except for the fermion gauge charge assignments: In the Simmons and Popovic model, the fermions are treated flavor universal in the $SU(3)$ sector, but *not* in the $U(1)$ sector. Table 4.1 shows the gauge charge assignments in this model and should be compared to table 2.1. The important dif-

	$SU(N)_{TC}$	$SU(3)_1$	$SU(3)_2$	$SU(2)_W$	$U(1)_1$	$U(1)_2$
I	1	SM	1	SM	0	SM
II	1	SM	1	SM	0	SM
III	1	SM	1	SM	SM	0

Table 4.1. Gauge charge assignments for fermions of I, II and III generation in the Simmons and Popovic model. "SM" indicates assignment corresponding to the Standard Model. Compare to table 2.1.

ference to the Topcolor model we considered so far is of course the flavor non-universal $U(1)$ sector. Due to this flavor-non-universality, we can not calculate the electroweak parameters $\widehat{S}$, $\widehat{T}$, ... Nevertheless, our derivation of the shift in the Z boson coupling in section 2.5 was general enough to also cover this model: We simply have to use the general expression for the Z coupling from eqn. (2.50):

$$g_Z = \frac{e}{\sin\theta\cos\theta}\left[T^3 - Q\sin^2\theta - x^2\left(Y_1 - \sin^2\phi Y\right)\left(\cos^2\alpha - \cos^2\phi\right)\right] \qquad (4.1)$$

All other considerations, including the W mass shift, are independent of setting $Y = Y_1$ in the flavor universal case. Using the Z coupling of eqn. (4.1) and using the fermion charge

assignments of table 4.1, we see that in the Simmons and Popovic model the corrections to the Standard Model for third generation fermions are proportional to $\cos^2\phi$ as was true for all fermions in the Topcolor model we considered in the preceding chapters. On the other hand, the first and second generation particles will result in a correction proportional to $\sin^2\phi$. This is all we need to know to do a combined fit to all 19 flavor universal observables listed in Fig. 4.1 and in the appendix.

The resulting fit is very bad, with a $\chi^2_{\text{min}}/\text{d.o.f.} = 48.5/(19-2) = 2.9$ for the best fit values $\cos^2\phi = 0$ and $x^2 = 0.0015$ (where we again searched for the global minimum just in the physical region where $x^2 \geq 0$ and $0 \leq \cos^2\phi \leq 1$ and fixed $f_t \approx 75$ GeV). Fig. 4.1 illustrates the fitting result by again showing the pulls of each observable.

Since all LEP measurements are in compliance with the assumption of lepton universality, it is not surprising that a model with a flavor non-universal hypercharge sector is more likely to run into problems than a universal one. The best fit value of $\cos^2\phi = 0$ forces us to a region in the parameter space where $\sin^2\phi$ is close to one. This results in large contributions coming from corrections due to the first and second generation fermions. It is likely that this spoils the fit.

We conclude that based on the preceding analysis, the Simmons and Popovic Topcolor model seems to be ruled out. Of course we should note that we again did not take into account implications of ETC (for example, the shift in the Z boson coupling due to ETC, which also would depend on the particular ETC model under consideration).

The same arguing can be made for another Topcolor assisted Technicolor model which treats both, the hypercharge sector and the Coloron sector flavor non-universal and was proposed by Christopher Hill [10].

Without question, the bottom line seems to be that Topcolor assisted Technicolor models with flavor universal hypercharge sectors are more favorable.

Experimental Value	Fit	Pull
Γ_Z= (2.4952±0.0023) GeV	2.4894 GeV	
σ_{had}= (41.541±0.037) nb	41.4574 nb	
R_e= 20.804±0.050	20.7466	
R_μ= 20.785±0.033	20.7468	
R_τ= 20.764±0.045	20.7501	
A^e_{FB}= 0.0145±0.0025	0.0166	
A^μ_{FB}= 0.0169±0.0013	0.0166	
A^τ_{FB}= 0.0188±0.0017	0.0158	
A^τ_{LR}= 0.1465±0.0033	0.1417	
A^e_{LR}(SLD)= 0.1516±0.0021	0.1493	
A^μ_{LR}(SLD)= 0.142±0.015	0.1493	
A^τ_{LR}(SLD)= 0.136±0.015	0.1417	
M_W= (80.403±0.029) GeV	80.3035 GeV	
R_b= 0.21629±0.00066	0.2160	
R_c= 0.1721±0.0030	0.1722	
A^b_{FB}= 0.0992±0.0016	0.1046	
A^c_{FB}= 0.0707±0.0035	0.07491	
A^b_{LR}= 0.923±0.020	0.9343	
A^c_{LR}= 0.670±0.027	0.6693	

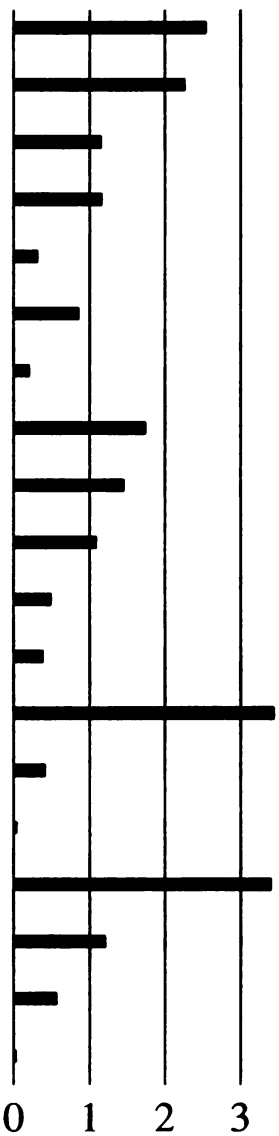

Figure 4.1. Comparison of the experimental values and the best fit prediction of the flavor non-universal Topcolor model corresponding to a χ^2_{min}/d.o.f. = 48.5/(19 − 2) = 2.9 using a Higgs mass of 800 GeV. Also shown is the pull of each measurement, which is defined as the difference between measurement and expectation over the uncertainty of the measurement.

Chapter 5

Conclusions

Our analysis shows that the dominating constraints on Topcolor assisted Technicolor models come from electroweak precision measurements. In the case of the Simmons and Popovic model with the flavor non-universal hypercharge sector, these constraints are strong enough to make the model highly unsatisfactory.

In the case of the Topcolor model with the flavor universal hypercharge sector, we are able to fit the electroweak data well. But we are forced to a rather high scale around 5 TeV, which, in the NJL model approximation, results in some fine tuning of the coupling constants κ_1 and κ_3, because they are forced to lie very close to their critical values in order to be able to produce a dynamical top mass of around 170 GeV, which is much smaller than the scale.

We were also able to estimate the gauge boson masses of the Z' and the Coloron due to our constraint from the LEP2 data. The Z' mass $M_{Z'}$ is bound to be $M_{Z'} \gtrsim 2$ TeV. The best fit value, though, would correspond to the limit $M_{Z'} \to \infty$. Since we are forced to a rather large $M_{Z'}$ and κ_1 being small, the contact interaction constraint we considered in section 3.2 does not give us additional bounds on the Z' mass. Analogously, the Coloron mass was estimated to lie between 20 and 30 TeV due to electroweak constraints. This is much heavier than the lower bound we found on the Coloron mass in section 3.1 from the requirement to have sufficiently suppressed flavor changing neutral currents, which naturally arise in every Topcolor model due to the non-flavor universal treatment of the

third generation. We are thus able to fulfill all experimental bounds we checked.

One unsatisfactory feature of the model we discussed is the unspecified first symmetry breaking at the scale u. Of course, we do not want to introduce an elementary scalar acquiring a non-zero vev like in the SM. After all, it was one of the main motivations to introduce Technicolor to get rid of the elementary Higgs of the SM. Unfortunately the scale u is so high that there is no obvious way to break that symmetry through a Technicolor condensate which is assumed to form at a much lower scale of around $v \approx 250$ GeV.

In the future, with the LHC (Large Hadron Collider), there will be various more things to look at. For example possible signatures of Z' decaying to quarks or leptons. Of course, a discovery of a Higgs particle, which couples like predicted by the SM would immediately rule out (Topcolor assisted) Technicolor models like the one we considered here.

It would also be interesting to do one-loop calculations in this model like it has been done for the three-site model in ref. [13] and to see whether the experimental bounds can still be fulfilled.

APPENDICES

Appendix A

Experimental Data and SM Predictions Used In Our Analysis

Observable	$M_H = 800$ GeV	$M_H = 1500$ GeV
Γ_Z [GeV]	2.488069	2.485958
σ_{had} [nb]	41.4881	41.4887
R_e	20.715	20.7118
R_μ	20.715	20.7121
R_τ	20.721	20.7589
A_{FB}^e	0.01444	0.01411
A_{FB}^μ	0.01444	0.0144
A_{FB}^τ	0.01444	0.0144
M_W [GeV]	80.23222	80.20057
A_{LR}^e	0.1388	0.1372
A_{LR}^μ	0.1388	0.1372
A_{LR}^τ	0.1388	0.1372
$\mathcal{P}_\tau$	0.1388	0.1372
R_b	0.2158	0.2159
R_c	0.1722	0.1722
A_{LR}^b	0.9340	0.9340
A_{LR}^c	0.6642	0.6635

Table A.1. ZFITTER SM prediction for two different Higgs masses. For the asymmetries additionally the ZFITTER based program SMATASY [12] was used. The ZFITTER and SMATASY input parameters are given in table A.7.

$\Gamma_Z = (2.4952 \pm 0.0023)$ GeV	total Z width
$\sigma_{\rm had} = (41.540 \pm 0.037)$ nb	$e\bar{e}$ hadronic cross section
$R_\ell = 20.767 \pm 0.025$	$\Gamma(Z \to \text{hadrons})/\Gamma(Z \to \ell^+\ell^-)$
$A^\ell_{FB} = 0.01714 \pm 0.00095$	Forward/Backward asymmetry in $e\bar{e} \to \ell\bar{\ell}$
$M_W = (80.426 \pm 0.034)$ GeV	pole W mass
$\mathcal{P}_\tau = 0.1465 \pm 0.0032$	τ polarization
$A^\ell_{LR} = 0.1513 \pm 0.0021$	Left/Right asymmetry in $e\bar{e} \to \ell\bar{\ell}$ (SLD)
$R_b = 0.21644 \pm 0.00065$	$\Gamma(Z \to b\bar{b})/\Gamma(Z \to \text{hadrons})$
$R_c = 0.1718 \pm 0.0031$	$\Gamma(Z \to c\bar{c})/\Gamma(Z \to \text{hadrons})$
$A^b_{FB} = 0.099 \pm 0.0017$	Forward/Backward asymmetry in $e\bar{e} \to b\bar{b}$
$A^c_{FB} = 0.067 \pm 0.0026$	Forward/Backward asymmetry in $e\bar{e} \to c\bar{c}$
$A^b_{LR} = 0.922 \pm 0.02$	Left/Right asymmetry in $e\bar{e} \to b\bar{b}$
$A^c_{LR} = 0.670 \pm 0.026$	Left/Right asymmetry in $e\bar{e} \to c\bar{c}$
$M_Z = 91.1875$ GeV	pole Z mass
$m_h > 114$ GeV	Higgs mass
$G_{\rm F} = 1.16637\,10^{-5}$ GeV^{-2}	Fermi constant for μ decay
$m_t = (178.0 \pm 4.3)$ GeV	pole top mass
$\alpha_{\rm s}(M_Z) = 0.118 \pm 0.003$	strong coupling
$\alpha^{-1}_{\rm em}(M_Z) = 128.949 \pm 0.046$	electromagnetic coupling
$Q_W = -72.83 \pm 0.49$	atomic parity violation in Cs
$A_{\rm PV} = (-160 \pm 27)\,10^{-9}$	Møller scattering at $Q^2 = 0.026$ GeV^2

Table A.2. The high and low-energy precision data included in the Barbieri et al. fit [2]. Barbieri et al. also used LEP2 measurements of the following cross-sections: $e\bar{e} \to e\bar{e}, \mu\bar{\mu}, \tau\bar{\tau}, \sum_q q\bar{q}$ at $\sqrt{q^2} \approx 189, 192, 196, 200, 202, 205, 207$ GeV.

Experimental Value	Γ_Z	$\sigma_{\rm had}$	R_ℓ	A^ℓ_{FB}
$\Gamma_Z = (2.4952 \pm 0.0023)$ GeV	1.000			
$\sigma_{\rm had} = (41.540 \pm 0.037)$ nb	-0.297	1.000		
$R_\ell = 20.767 \pm 0.025$	0.004	0.183	1.000	
$A^\ell_{FB} = 0.0171 \pm 0.0010$	0.003	0.006	-0.056	1.000

Table A.3. Experimental values from [6], with corresponding correlation matrix. Assuming lepton universality.

Experimental Value	Γ_Z	$\sigma_{\rm had}$	R_e	R_μ	R_τ	A^e_{FB}	A^μ_{FB}	A^τ_{FB}
$\Gamma_Z = (2.4952 \pm 0.0023)$ GeV	1.000							
$\sigma_{\rm had} = (41.541 \pm 0.037)$	-0.297	1.000						
$R_e = 20.804 \pm 0.050$	-0.011	0.105	1.000					
$R_\mu = 20.785 \pm 0.033$	0.008	0.131	0.069	1.000				
$R_\tau = 20.764 \pm 0.045$	0.006	0.092	0.046	0.069	1.000			
$A^e_{FB} = 0.0145 \pm 0.0025$	0.007	0.001	-0.371	0.001	0.003	1.000		
$A^\mu_{FB} = 0.0169 \pm 0.0013$	0.002	0.003	0.020	0.012	0.001	-0.024	1.000	
$A^\tau_{FB} = 0.0188 \pm 0.0017$	0.001	0.002	0.013	-0.003	0.009	-0.020	0.046	1.000

Table A.4. Experimental values from [6], with corresponding correlation matrix. *Without* lepton universality.

Experimental Value	A^e_{LR}	A^μ_{LR}	A^τ_{LR}
$A^e_{LR} = 0.1516 \pm 0.0021$	1.000		
$A^\mu_{LR} = 0.142 \pm 0.015$	0.038	1.000	
$A^\tau_{LR} = 0.136 \pm 0.015$	0.033	0.007	1.000
$A^\ell_{LR} = 0.1513 \pm 0.0021$			
$M_W = (80.403 \pm 0.029)$ GeV			
$\mathcal{P}_\tau = 0.1465 \pm 0.0033$			

Table A.5. Experimental values from [6] and [16]. The first left/right asymmetry values with and without lepton universality were measured by SLD and are given in ref. [6]. The last asymmetry, $\mathcal{P}_\tau$, value was used in both fits and corresponds to direct LEP measurement of the τ-polarization. Compared to the W mass given in ref. [6], we use the more recent value (updated by Tevatron measurements) given in ref. [16].

Experimental Value	R_b	R_c	A^b_{FB}	A^c_{FB}	A^b_{LR}	A^c_{LR}
$R_b = 0.21629 \pm 0.00066$	1.00					
$R_c = 0.1721 \pm 0.0030$	-0.18	1.00				
$A^b_{FB} = 0.0992 \pm 0.0016$	-0.10	0.04	1.00			
$A^c_{FB} = 0.0707 \pm 0.0035$	0.07	-0.06	0.15	1.00		
$A^b_{LR} = 0.923 \pm 0.020$	-0.08	0.04	0.06	-0.02	1.00	
$A^c_{LR} = 0.670 \pm 0.027$	0.04	-0.06	0.01	0.04	0.11	1.00

Table A.6. Experimental values from [6], with corresponding correlation matrix.

$\alpha_s(M_Z) = 0.1176 \pm 0.0020$	strong coupling
$\Delta\alpha^5_{\rm had}(M_Z) = 2.8040$	hadronic vacuum polarization
$\alpha^{-1}_{em}(M_Z) = 128.949 \pm 0.046$	electromagnetic coupling
$G_F = (1.16637 \pm 0.00001)\, 10^{-5}$	Fermi constant [GeV^{-2}]
$M_Z = 91.1876 \pm 0.0021$ GeV	pole Z mass
$m_t = 174.2 \pm 3.3$ GeV	top quark mass

Table A.7. From ref. [16]: The high energy precision data used as input parameters in our analysis (i.e. held fixed during fitting). Except for $\alpha_{em}(M_Z)$, these are also the ZFITTER input parameters. The given value for the electromagnetic coupling constant at the Z-pole is calculated by ZFITTER in dependence on $\Delta\alpha^5_{\rm had}$.

Appendix B

The Conjugate Representation

A representation $R = \exp(i\alpha^a T^a)$ of the group $SU(N)$, where T^a are the corresponding hermitean group generators, applied to a vector ψ yields the infinitesimal transformation

$$\psi \to (1 + i\alpha^a T^a)\,\psi. \tag{B.1}$$

Now for each transformation generator T^a, there is a generator $(T^a)^* = (T^a)^T$ belonging to the associated conjugate representation, since

$$\psi^* \to \left(1 - i\alpha^a\,(T^a)^*\right)\psi^*. \tag{B.2}$$

If there is a unitary transformation connecting these two sets of generators, the representation R is called real, otherwise equation (B.2) defines the conjugate representation of equal dimension, denoted $\bar{R}$.

It is now useful to define

$$\psi^i \equiv \psi_i^*, R_i{}^j \equiv R_{ij} \text{ and } R^i{}_j \equiv R_{ij}^*. \tag{B.3}$$

Then our transformations (B.1) and (B.2) read

$$\begin{aligned} \delta\psi_i &= +i\alpha^a\,(T^a)_i^j\,\psi_j \\ \delta\psi^i &= -i\alpha^a\,(T^a)_j^i\,\psi^j, \end{aligned} \tag{B.4}$$

where the hermicity of T^a was used: $(T^a)_i{}^j = (T^a)^j{}_i \equiv (T^a)_i^j$.

Bibliography

Bibliography

[1] A. B. Arbuzov, M. Awramik, M. Czakon, A. Freitas, M. W. Gruenewald, K. Moenig, S. Riemann, and T. Riemann. Zfitter: a semi-analytical program for fermion pair production in e+e- annihilation, from version 6.21 to version 6.42. *Computer Physics Communications*, 174:728, 2006.

[2] Riccardo Barbieri, Alex Pomarol, Riccardo Rattazzi, and Alessandro Strumia. Electroweak symmetry breaking after lep1 and lep2. *Nuclear Physics B*, 703:127, 2004.

[3] Ta-Pei Cheng and Ling-Fong Li. *Gauge Theory of Elementary Particle Physics*. Oxford University Press, 2005.

[4] R. Sekhar Chivukula. Electroweak parameters in $SU(2) \times U(1)^2$ triangle moose. *unpublished*, 2007.

[5] R. Sekhar Chivukula, Hong-Jian He, Masafumi Kurachi, Elizabeth H. Simmons, and Masaharu Tanabashi. Universal non-oblique corrections in higgsless models and beyond. *Physics Letters B*, 603:210, 2004.

[6] The LEP Collaborations: Aleph collaboration, DELPHI Collaboration, L3 Collaboration, OPAL Collaboration, and the LEP Electroweak Working Group. A combination of preliminary electroweak measurements and constraints on the standard model. 2006.

[7] E. Farhi. An introduction to symmetry breaking in the standard model. Prepared for Theoretical Advanced Study Institute in Elementary Particle Physics (TASI 91): Perspectives in the Standard Model, Boulder, CO, 2-28 Jun 1991.

[8] H. Georgi. A tool kit for builders of composite models. *Nucl. Phys.*, B266:274, 1986.

[9] Christopher T. Hill. Topcolor: Top quark condensation in a gauge extension of the standard model. *Phys. Lett.*, B266:419–424, 1991.

[10] Christopher T. Hill. Topcolor assisted technicolor. *Phys. Lett.*, B345:483–489, 1995.

[11] Christopher T. Hill and Elizabeth H. Simmons. Strong dynamics and electroweak symmetry breaking. *Phys. Rept.*, 381:235–402, 2003.

[12] S. Kirsch and T. Riemann. Smatasy - a program for the model independent description of the z resonance. *Computer Physics Communications*, 88:89, 1995.

[13] Shinya Matsuzaki, R. Sekhar Chivukula, Elizabeth H. Simmons, and Masaharu Tanabashi. One-loop corrections to s-parameter in a three site higgsless model. *Phys. Rev.*, D75:073002, 2007.

[14] Marko B. Popovic and Elizabeth H. Simmons. A heavy top quark from flavor-universal colorons. *Physical Review D*, 58:095007, 1998.

[15] Koichi Yamawaki. Dynamical symmetry breaking with large anomalous dimension. 1996.

[16] W. M. Yao et al. Review of particle physics. *J. Phys.*, G33:1–1232, 2006.